Journal of Hydrology 632 (2024) 130698

Contents lists available at ScienceDirect

Journal of Hydrology

journal homepage: www.elsevier.com/locate/jhydrol

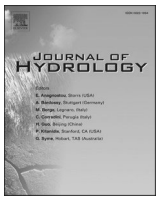

Research papers

A watershed-scale multi-approach assessment of design flood discharge estimates used in hydrologic risk analyses for forest road stream crossings and culverts

Sourav Mukherjee [a,*], Devendra M. Amatya [a], John L. Campbell [b], Landon Gryczkowski [c], Sudhanshu Panda [d], Sherri L. Johnson [e], Kelly Elder [f], Anna M. Jalowska [g], Peter Caldwell [h], Johnny M. Grace [i], Dariusz Młyński [j], Andrzej Wałęga [j]

[a] Center for Forested Wetlands Research, Southern Research Station, USDA Forest Service, 3734 Highway 402, Cordesville, SC 29434, USA
[b] Northern Research Station, USDA Forest Service, Durham, NH, USA
[c] Northern Research Station, USDA Forest Service, NH, USA
[d] Institute of Environmental Spatial Analysis, University of North Georgia, 3820 Mundy Mill Road, Oakwood, GA 30566, USA
[e] Pacific Northwest Research Station, USDA Forest Service, Corvallis, OR, USA
[f] Rocky Mountain Research Station, USDA Forest Service, Fort Collins, CO, USA
[g] Office of Research and Development, U.S. Environmental Protection Agency, Research Triangle Park, NC, USA
[h] Center for Forest Watershed Research, Southern Research Station, USDA Forest Service, 3160 Coweeta Lab Rd, Otto, NC 28763, USA
[i] Center for Forest Watershed Research, Southern Research Station, USDA Forest Service, 1740 S. Martin, USA
[j] Department of Engineering Sanitary and Water Department, University of Agriculture in Krakow, Mickiewicza 6 21, 31-120 Krakow, Poland

ARTICLE INFO

This manuscript was handled by Emmanouil Anagnostou, Editor-in-Chief

Keywords:
Flood risk
Nonstationary regional frequency analysis
Hydrologic vulnerability of culvert
Forest service experimental forests
Headwater catchments
Road-stream crossing structures

ABSTRACT

Flood peak magnitudes and frequency estimates are key components of any effective nationwide flood risk management and flood damage abatement program. In this study, we evaluated normalized peak design discharges (Q_p) for 1,387 hydrologic unit code 16 to 20 (HUC16-20) watersheds in the White Mountain National Forest (WMNF), New Hampshire and in five Experimental Forest (EF) regions across the United States managed by USDA Forest Service (USDA-FS). Nonstationary regional frequency analysis (RFA) and single site frequency analysis (FA) with long-term high-resolution observed streamflow data along with the deterministic Rational Method (RM) and semi-empirical United States Geological Survey regional regression equation (USGS-RRE) were used. Additionally, a hydrologic vulnerability assessment was performed for 194 road culverts as a result of extreme precipitation-induced flooding on gauged and ungauged watersheds in the Hubbard Brook EF (HBR) within the WMNF. The RM outperformed the USGS-RRE in predicting Q_p in the gauged and ungauged HUC16-20 watersheds of WMNF and in three other small, high-relief forest headwater watersheds—Coweeta Hydrologic Lab EF's watershed-14, and watershed-27 in North Carolina and HJ Andrews EF's watershed 8 in Oregon. However, the USGS-RRE performed better for larger watersheds, such as the Fraser EF's St. Louis watershed in Colorado and the Santee EF's watershed 80 in South Carolina. About 31 %, 26 %, and 56 % of the culverts at the HBR site could not accommodate the 100-yr Q_p estimated by RFA, RM and USGS-RRE, respectively. Based on the chosen RIs and techniques, it is determined that except for one culvert with diameter = 0.91 m (36 in.), none of the culverts with diameter of 0.75 m (30 in.) or larger are hydrologically vulnerable. Our results suggest that the observation based RFA works best where multiple gauges are available to extrapolate information for ungauged watersheds, otherwise, RM is best-suited for smaller headwater watersheds and USGS-RRE for larger watersheds. Results from the hydrologic vulnerability analysis revealed that replacing undersized culverts with new culverts of diameter $\geq$ 0.75-m will improve flood resiliency, provided that the structure is geomorphologically safe (with minimal effects of debris flow, erosion, and sedimentation) and allows for both bank-full discharge and necessary fish passage within that design limit. This study has implications in managing road culverts and crossings at Forest Service and other forested lands for their resiliency to extreme precipitation and flooding hazards induced by climate change.

* Corresponding author.
E-mail address: sourav.mukherjee@usda.gov (S. Mukherjee).

https://doi.org/10.1016/j.jhydrol.2024.130698
Received 5 September 2023; Received in revised form 14 December 2023; Accepted 17 December 2023
Available online 29 January 2024
0022-1694/Published by Elsevier B.V.

1. Introduction

Extreme precipitation and floods emerge as the foremost threat to road culvert systems, surpassing other climate change-related hazards due to their capacity to cause damage and disrupt transportation networks (Pregnolato et al., 2017; USDOT, 2018; Amatya et al., 2021a–c; Darestaniet al., 2021). Floods can significantly alter hydrological processes, and cause soil erosion and landslides, having devastating impacts on forest road infrastructure and ecosystems (Mishra et al., 2022; Panda et al., 2022; Goodman et al., 2023). The flooding events that occur after extreme precipitation events has been reported in regions all over the globe (Papalexiou and Montanari, 2019). Over the last few decades, intensity and the frequency of rainfall events leading to floods have increased, which has affected Experimental Forest (EF) regions and National Forest lands managed by the US Department of Agriculture Forest Service (USDAFS) (Amatya et al., 2016; Glasser, 2005). For example, the September 2013 flood that occurred in the Roosevelt and Arapaho National Forests in Colorado affected numerous roads and trails, destroyed bridges and culverts, and claimed several lives (Gochis et al., 2015). The October 2015 flooding caused by unprecedented rainfall in the Francis Marion National Forest in South Carolina damaged culverts and roads, and inundated gauging stations (Amatya et al., 2016; Marciano and Lackmann, 2017), and altered the ecology of the forest (Van Dam et al., 2018; Mishra et al., 2021). The flooding breached dams and roads causing substantial erosion and sedimentation that may have long-term effects on water quality and aquatic habitats (Magilligan et al., 2019). Tropical storm Irene in August 2011, resulted in heavy rain and flash flooding in the Hubbard Brook National Forest in New Hampshire, which damaged culverts and bridges and made some roads impassable, blocking access to some areas for weeks to months (Olson and Bent, 2013; Yellen et al., 2016). The H.J. Andrews Experimental Forest in the Cascade Range of western Oregon has also experienced periodic flooding, including a major flood in 1996 (Chang et al., 2010; Johnson et al., 2000). The increased likelihood of extreme precipitation events under a changing climate is projected to cause substantial increases in the magnitude and frequency of floods, including those caused by hurricanes and tropical storms (Berghuijs et al., 2016).

The profound effect of flooding on forest ecosystems and infrastructure has highlighted the need for greater resilience of forest land to extreme precipitation events (Keller and Sherar, 2003; Keller and Ketcheson, 2011). Road stream crossing structures (RSCS), such as road lead off structures, fords, culverts, and bridges play a crucial role in the national forests' road network (Keller and Sherar, 2003). This system is essential for sustainable management, which involves, balancing the demands of resource management and traffic with the preservation of aquatic habitats and ecosystem health (Seddon et al., 2021). The hydrologic risk from flooding is amplified with inadequately sized RSCS, and together with soil erosion and flooding, can cause structural failures that leads to financial losses and disturb stream connectivity essential for aquatic organism passage (Heredia et al., 2016). Many RSCS, specifically culverts on the forest lands, are currently deemed undersized for accommodating bank-full flow conditions for 1- to 2-year flooding, which is one of the critical design considerations required for flood resiliency (USDOT, 2018; Amatya et al., 2021a–c).

Deterministic and empirical methods, such as, the Rational Method (RM) (Kuichling, 1889) and Natural Resource Conservation Service (NRCS) Graphical Peak Discharge method (GPDM) (USDA, 2021) have been widely used for estimating flood peak discharges, especially, in small to medium-sized watersheds or rural areas where hydrologic data may be limited (Fleming and Franz, 1971; Walder and O'Connor, 1997; Megnounif et al., 2013; Amatya et al., 2021a–c). However, it is important to note that deterministic methods have limitations and are not appropriate in all situations, especially complex hydrologic terrain (Grimaldi and Petroselli, 2015a,b; Grimaldi et al., 2021). Their accuracy depends on the quality and quantity of data used to develop the method and requires an accurate calibration of parameters (Montanari and Koutsoyiannis, 2014), which is expensive and time-consuming task (Ke et al., 2020). Amatya and Walega (2020) suggest validating these methods, their modified versions, and their parameters with long-term hydroclimatic data from a range of watersheds.

Estimating flood peak discharge with USGS Regional Regression Equations (USGS-RREs) is a semi-empirical approach that accounts for various factors that influence flooding, such as the size of the drainage area, topography, the type of soil, and precipitation magnitude (e.g., average 24-hr maximum precipitation) in some cases (Vogel et al., 1999; Capesius and Stephens, 2009). As such, simple linear and multivariate regressions of the record peak discharges as a function of drainage area (and additional regional predictors) are widely used for estimating flood frequency as well as predicting, ranking, and defining expected flood magnitudes for medium to large watersheds (Yochum et al., 2019; Levin and Sanocki, 2023). Although this method has proved useful, there are several limitations including: 1) poor performance when there is limited data available for developing the regression equations, 2) limited applicability to regions with complex hydrological conditions, 3) lack of consideration of factors such as land use change, antecedent moisture conditions and climate variability to predict flood peaks, and 4) high uncertainty associated with predicting flood peaks outside the range of available data, and associated assumptions, such as stationarity of the data used to develop the regression equations (Mitchell et al., 2023; Amatya et al., 2021a–c). Various studies (Amatya et al., 2021a–c; Marion, 2004; Thompson, 2006; Trommer et al., 1996) have shown that the USGS-RRE has a tendency to overestimate design discharge for small undisturbed watersheds. Additionally, extrapolating to smaller watersheds outside the boundaries of the regression data can be problematic (Genereux, 2003).

In comparison to deterministic and semi-empirical methods like the RM and the USGS-RREs, probability-based flood frequency analysis (Vogel and Castellarin, 2017; Read and Vogel, 2015) is usually considered a more rigorous and robust technique for flood peak estimation (Mishra et al., 2022). This is particularly true for complex watersheds where the assumptions of hydrological models may not hold (Thompson, 2004). In addition, probability-based techniques involve statistical analysis of historically observed data and unlike the other methods, take into consideration the variability of flood events over time (Pegram and Parak, 2004). One of the major benefits of probability-based flood frequency analysis is that it can be used to analyze extreme events that might not have happened during the observed record of flood data, particularly in intermittent streams (Mishra et al., 2022). Based on the probability distribution, the likelihood of extreme events happening in the future can be estimated, which is critical in designing climate resilient infrastructure to manage flood risk. Furthermore, probability-based regional frequency analysis (RFA) is more reliable in transferring flood information from gauged to ungauged watersheds (Gaume et al., 2010). RFA considers the regional variations in hydrologic characteristics that effect flood frequency estimates, and is, therefore, a more sophisticated technique for flood frequency analysis compared to flood frequency analysis considering a single site (hereafter referred to as FA) (Halbert et al., 2016). More specifically, a RFA, that incorporates non-stationary covariates such as hydro-geomorphic (Rootzén and Katz, 2013; Wasko et al., 2020; De Michele and Salvadori, 2002; Mishra et al., 2022) and climatic conditions (Mishra et al., 2022) is more wholistic, and can be extended to predict flood peaks in similar but ungauged watersheds (Kim et al., 2020). Though these factors play an important role in flooding, they are currently under-represented in existing deterministic and semi-empirical models reported in the literature (Teng et al., 2017).

Precipitation-intensity–duration–frequency (PIDF) estimates of storm events can also be helpful for determining how frequently floods may harm RSCS causing traffic disruption and erosion in road networks and headwater valleys (Jakob et al., 2020; 2022; Mamo, 2015). The majority of RSCS on USDA-FS land are in small drainage areas (<1000 ha or 10 km^2) with forested headwater watersheds, typically with sub-

daily time of concentrations (*Tc*) (USDA, 2021; Amatya et al., 2021a–c; Corbin et al., 2021; Yochum et al., 2019; Walega et al., 2020). Therefore, it is most likely that flood potential in small watersheds will be underestimated if design flow rates are calculated using PIDF estimates at a daily timescale with limited period-length integrated to an event-based approach (Viglione and Blöschl, 2009; Wright et al., 2019; Mukherjee et al., 2023; Amatya et al., 2021a–c). Synthetic rainfall generation models coupled with continuous rainfall-runoff transformation in data scares conditions can provide a more accurate representation of rainfall events in hydrological models (Beven, 2011; Pathiraja et al., 2012; Winter et al., 2019; Beneyto et al., 2020; Grimaldi et al., 2022). However, its use remains limited due to the challenges in selecting the optimal rainfall simulation model for specific risk analysis needs (Grimaldi et al., 2022). As such, due to a lack of long-term historical precipitation records at a fine temporal resolution (sub-hourly and sub-daily timescales), the RSCS on USDA-FS lands and other similar landscapes are typically designed using coarser, daily resolution or, if available, the sub-hourly and sub-daily PIDFs provided by the National Oceanic and Atmospheric Administration (NOAA) Atlas 14 which has multiple caveats (Mukherjee et al., 2023; Perica et al., 2018). Multiple studies have shown that as an alternative to the NOAA data, the USDA-FS EF's long-term, sub-hourly to sub-daily PIDFs that are available at some sites, can be used to determine reliable estimates of design discharge for the small EF watersheds (Amatya and Walega, 2020; Amatya et al., 2021a–c; Mukherjee et al., 2023).

In this study, we used USDA-FS EF's long-term, high-resolution precipitation intensities and instantaneous streamflow records to determine the hydrologic vulnerability of RSCS to overtopping on national forest and multiple EF lands that represent a range of climatic conditions. We applied several approaches and methods including, probability-based stationary and nonstationary FA and RFA that requires gauged streamflow data, and deterministic and semi-empirical methods like RM, and USGS-RRE, respectively, for estimating the normalized peak design discharge (Q_p). These methods are extensively used by engineers and land managers to perform flow analysis, determining design size of culverts, and identifying the most realistic hydrologic risk for the drainage crossings located on forested watersheds (Keller and Sherar, 2003; Keller and Ketcheson, 2011). RFA, RM, and USGS-RRE were implemented for estimating Q_p for micro-scale watersheds at the White Mountain National Forest (WMNF) region and the Hubbard Brook EF (HBR) within the WMNF region in New Hampshire, and the HJ Andrews EF (HJA) in Oregon. Similarly, FA, RM and USGS-RRE were used to estimate Q_p for gauged watersheds in multiple other EFs including the Coweeta Hydrological Laboratory (CHL), Fraser (FRS), and Santee (SAN). The performance of the deterministic methods was evaluated against the results from the RFA and FA, which is important because of the limitations of the deterministic approaches in estimating flood discharge in the complex, heterogeneous micro watersheds. In this pilot study, we estimated the hydrological vulnerability of culverts to flooding for road culverts in the ungauged and gauged micro watersheds in the HBR EF.

The current study is the first multi-site hydrologic risk assessment of road culverts demonstrating a holistic approach using sub-daily/sub-hourly hydro-climatic data to assess flood-induced risk of culvert failure in small, forested headwater catchments across diverse US climate regions. Employing a novel multi-approach framework, it presents the first comprehensive evaluation of these risks, integrating non-stationary regional flood frequency analysis, and associated uncertainties and deviance from deterministic and empirical assessments with culvert hydraulics assessment. The findings from the study will have important implications for managing and restoring road culverts and crossings in forested lands, enhancing their resilience to extreme precipitation and climate-induced flooding.

2. Data and methodology

2.1. Data

The hydrological vulnerability assessment of the RSCS involves two stages of analysis – (1) hydrologic analysis for estimating Q_p requiring multiple datasets including, hydrologic and meteorological dataset, and watershed geospatial dataset, and (2) estimation of culvert's hydraulic capacity (Q_c) that requires information on their georeferenced locations, dimensions, and type of culverts. Comparing the estimated flood discharge (=Q_p x watershed drainage area) for a design event of interest with the Q_c of the culvert allows assessment for the hydrological vulnerability of culvert to failure from overtopping. A complete step-by-step workflow of the data collection and processing, and the entire methodology used in the study is demonstrated in Fig. 1. A detailed information of the dataset used for the estimation of Q_p and hydrological vulnerability assessment of forest RSCS or culverts is given in the following sections.

2.1.1. Hydrologic and meteorological dataset

Long-term historical records of 15-min instantaneous streamflow and hourly and sub-hourly precipitation data were used to estimate design discharge for RSCS in one national forest, and five EFs: WMNF and HBR within the WMNF, New Hampshire; HJA, Oregon; SAN, South Carolina; CHL, North Carolina; and FRS, Colorado. Amatya et al. (2021a–c) and Harder et al. (2007) provide a detailed description of the study sites for SAN; Caldwell et al. (2016) and Laseter et al. (2012) for CHL; Likens (2013) and Campbell et al. (2021) for HBR; Johnson et al. (2021) and Fredriksen (1970) for HJA; and Alexander and Watkins (1977) for FRS. The USDA-FS's EF watersheds used in this study and their characteristics are provided in Table 1 along with the corresponding gauges and periods of data record. The spatial maps demonstrating the study watershed locations, boundaries, elevations, and stream channels are shown in Figs. 2–4.

Watersheds with a larger drainage area encompass a larger distributed channel system that generally drains into several road culverts simultaneously during a flood event. This may increase the uncertainty associated with linking the design discharge estimated for the watershed and the discharge capacity of any single culvert selected from amongst a network of multiple road culverts draining micro watersheds in the large watershed. Therefore, to minimize such uncertainties, we delineated the larger watersheds located within the WMNF (and HBR EF) boundary into micro watersheds, ranging between Hydrologic Unit Code 16 (HUC16) to HUC20, hereafter referred to as HUC16-20. The HUC16-20 watershed delineation was performed with Arc Hydro Tool in ESRI ArcGIS platform using the laser imaging, detection, and ranging (LiDAR) based 1-m digital elevation model (DEM) data (available at https://datagateway.nrcs.usda.gov/) (Likens, 2013; Campbell et al., 2021). It is important to note that, hereafter in this study, the delineated gauged watershed ID is referred by appending with "-d" to the USGS and USDA-FS's gauging station ID that drains out of the delineated watershed as shown in Table 2.

A total 1,387 road stream crossings (RSCs) within the WMNF were selected in the study (Fig. 2c). These RSCs were identified using the national hydrography dataset (Buto and Anderson, 2020). In the WMNF region we focused our analysis on the delineated watersheds (HUC16-20) that intersect with these 1,387 RSCs as shown in Fig. 2. The distribution of drainage area of these 1,387 micro watersheds is presented in Fig. 2f.

Historical 15-min instantaneous streamflow data were obtained from 10 USGS (Kiah and Stasulis, 2018) and four HBR's streamflow gauges (Table 2; Likens, 2013; Campbell et al., 2021) for the estimation of Q_p in the WMNF. For all other EFs, historical 15-min instantaneous streamflow data were obtained only from the USDA-FS streamflow gauging stations (Table 1). The 15-min instantaneous streamflow data were normalized by drainage area of the watersheds before using them in the

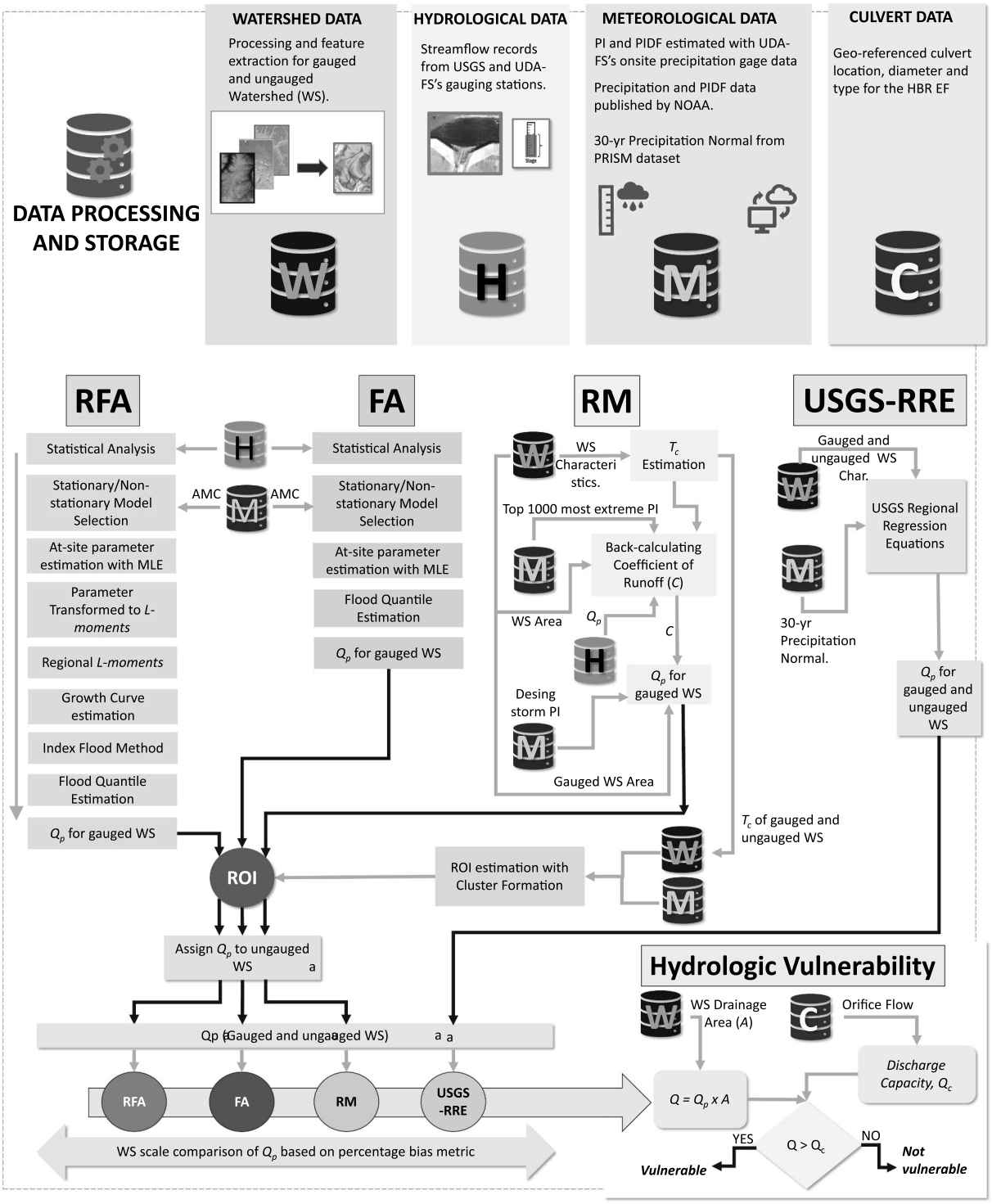

Fig. 1. Comprehensive workflow diagram demonstrating the data acquisition and methodology used in the study. Note that MLE indicates maximum likelihood estimation, *Tc* indicates time of concentration, RFA indicates Regional Frequency Analysis, FA indicates the single-site frequency analysis, RM indicates Rational Method, and USGS-RRE indicates the regional regression equations developed by USGS. The hydrologic vulnerability was assessed using each of the methodologies (i.e., RFA, FA, RM, and USGS-RRE), separately. RFA was applied to an EF region when data from more than two gauging sties were available, otherwise, FA was used to estimate the normalized peak design discharge (Q_p) for that EF watershed.

RFA, and FA to estimate Q_p. Long-term historical hourly and sub-hourly precipitation data and design storm PIs were obtained from the USDA-FS long term onsite rain gauges. 1-hour precipitation data were also obtained from the NOAA's rain gauges (available at https://www.ncei.noaa.gov/) that were closest to the USGS's streamflow gauges at the WMNF (Table 2) due to the unavailability of USDA-FS onsite rain gauges in the region. The hourly and sub-hourly precipitation data were used to estimate the antecedent soil moisture conditions and runoff coefficient (Table 2; see Methods) for the gauged watersheds. Annual average precipitation data for the period 1991–2020 was obtained from Parameter elevation Regression on Independent Slopes Model (PRISM; available at https://datagateway.nrcs.usda.gov/) for estimating Q_p with

Table 1
Characteristics of USDA-FS watersheds and streamflow gauging station selected in the study.

EF Name	Method Used	Streamflow Gauge ID/WS ID	Area (km^2)	Range of Elevation (m)	Mean basin slope (%)	Aspect	Period of complete flow record	Nearest long term rain gauge station
HBR	RFA, RM, & USGS-RRE	HBR-WS3	0.424	527–732	21.43	S23°W	1957–2021	RG01
		HBR-WS6	0.132	549–792	28.29	S32°E	1963–2021	RG01
		HBR-WS7	0.7738	619–899	21.98	N16°W	1965–2021	RG01
		HBR-WS8	0.594	610–905	24.93	N12°W	1968–2021	RG01
HJA	RFA, RM, & USGS-RRE	HJA-WS1	0.959	439–1027	59.35	NW	1951–2018	PRIMET
		HJA-WS8	0.204	962–1182	25.78	SE	1963–2018	H15MET
		HJA-WS9	0.085	438–731	58.36	SW	1968–2018	PRIMET
CHL	FA, RM, & USGS-RRE	CHL-WS14	0.6103	878	50	NW	1938–2015	CHL-RG41
		CHL-WS27	0.3905	1254	57	NE	1948–2015	CHL-RG31
SAN		SAN-WS80	2.06 and 1.55	3.5—–10	3	SE	1965–2020*	MET25
FRS		FRS-ELOUI	8.03	2895–3720	72	NW	1943–2021	FRS-HQTRS

*Note that the flow record for SAN-WS80 had missing data (period 1965–1968; and 1992–1995), which were filled with the flow record from adjacent watershed, WS77.

the USGS-RRE on the ungauged and gauged watersheds intersecting with RSC within the WMNF region.

The 25-year, 50-year, and 100-year precipitation intensities (PI) are generally used for estimating Q_p for designing forest drainage culverts and RSCS (Keller and Sherar, 2003; Keller and Ketcheson, 2011). In this study, the 25-year, 50-year, and 100-year PIs, published in Mukherjee et al., 2023, were used for estimating Q_p for USDA-FS's onsite rain gauges listed in Tables 1 and 2. In the WMNF, the 25-year, 50-year, and 100-year PI were obtained from the NOAA-Atlas14 (available at https://hdsc.nws.noaa.gov/pfds/?bkmrk=pa; Perica et al., 2015) due to the unavailability of USDA-FS's onsite gauges in the vicinity of the USGS gauging stations (Table 2). The PIs estimated with precipitation data from the onsite rain gauge station, RG01 were preferred over NOAA-gauges due to several shortcomings in the reliability of NOAA-Atlas14 published PIs for application in design discharge estimation within USDA-FS's EF lands (Amatya et al., 2021a–c; Mukherjee et al., 2023).

2.1.2. Watershed geospatial dataset

We used LiDAR based 1-m resolution DEM data (https://datagateway.nrcs.usda.gov/) to determine the watershed boundary and characteristics, such as slope, mean elevation, longest stream channel length, and topographic wetness index (Thomas et al., 2008; Sörensen et al., 2006) for the headwater watersheds within the WMNF and HBR. The application of 1-m LiDAR based DEM is preferred for representing the micro-watershed scale spatial variability of flood magnitudes for reducing uncertainty associated with the flood discharge estimates draining into any isolated road culvert out of a network of culverts located in small, forested headwater watersheds. 10-m DEM data (available at https://datagateway.nrcs.usda.gov/) were used for other EFs because 1-m LiDAR based DEM data were not available for some of them. However, we recognize that as a future extension of this work, 1-m LiDAR based DEM should be used for delineating these watersheds as and when the 1-m elevation and road culvert data becomes available for the culvert's hydrologic vulnerability assessment at these EF watersheds. Wetland cover data was obtained from the updated version of National Wetland Inventory (NWI) (available at https://www.fws.gov/program/national-wetlands-inventory/data-download), for calculating the percentage of wetland area within each watershed in the WMNF and HBR EF region. Hydrological soil group data was obtained from the Oak Ridge National Laboratory Distributed Active Archive Center (Ross et al., 2018) and was used to determine the average curve number (Boughton, 1989) in each watershed within the selected study regions.

2.1.3. Road stream crossing and culvert data

Roads and stream crossing (RSC) locations were obtained using the LiDAR based 1-m DEM data and primary and secondary roads data from the Census Bureau's Topologically Integrated Geographic Encoding and Referencing (TIGER) database (available at https://datagateway.nrcs.usda.gov/), Enterprise Data Warehouse of US Forest Service (available at https://www.fs.usda.gov/about-agency/enterprise-data-warehouse), and US Transit Roads (available at https://www.bts.gov/maps) for the WMNF region. The location of culverts was identified in GIS environment by using the Arc Hydro Tool and the national hydrography database for the USA (Buto and Anderson, 2020). A field survey was then conducted, and a database was developed, which included, longitude and latitude coordinates, diameter, construction material, and other related information for the 194 culverts in the HBR EF.

2.2. Nonstationary regional frequency analysis

Regional frequency analysis (RFA; Hosking and Wallis, 1997) combines observations of the same variable (here, the annual peak discharge) at various gauged streams to estimate hydrologic information that can be transferred from gauged to ungauged sites. RFA is primarily used to estimate peak flood discharge using the index-flood magnitude (Dalrymple, 1960; Hosking and Wallis, 1997) as a scaling factor of the adimensional flood frequency distribution, which is assumed to be the same for various sites in a homogeneous region. The RFA was performed with the index flood method using L-moments, where the quantile function, $Q_i(F)$ of the cumulative distribution function F at the i^{th} site (where $i = 1,2, \ldots, N$), is given as (Hosking and Wallis, 1997),

$$Q_i(F) = \mu_i q(F) \tag{1}$$

where, μ_i is the index-flood (scaling factor) calculated as the mean of the site-specific annual maximum series (AMS) of peak discharge, and $q(F)$ is adimensionless quantile function also known as the regional growth curve (or pooled growth function) estimated using the RFA. Once the regional growth curve was obtained for a region using the L-moment statistics, the site-specific quantiles were estimated with Eq. (1). Fig. 1 illustrates the workflow of the methodology used in the RFA.

2.2.1. Inclusion of non-stationary information

We employed the Block Maxima (BM) method to isolate the annual peak discharges. This method is generally applied in extreme value analysis to study the upper tail characteristics of hydrologic extremes (Coles et al., 2001) using a generalized extreme value distribution (GEV). The GEV is a three-parameter distribution comprising of the location (μ), scale (σ), and shape (ε) parameter, and the theoretical cumulative distribution function can be written following Coles et al. (2001) as,

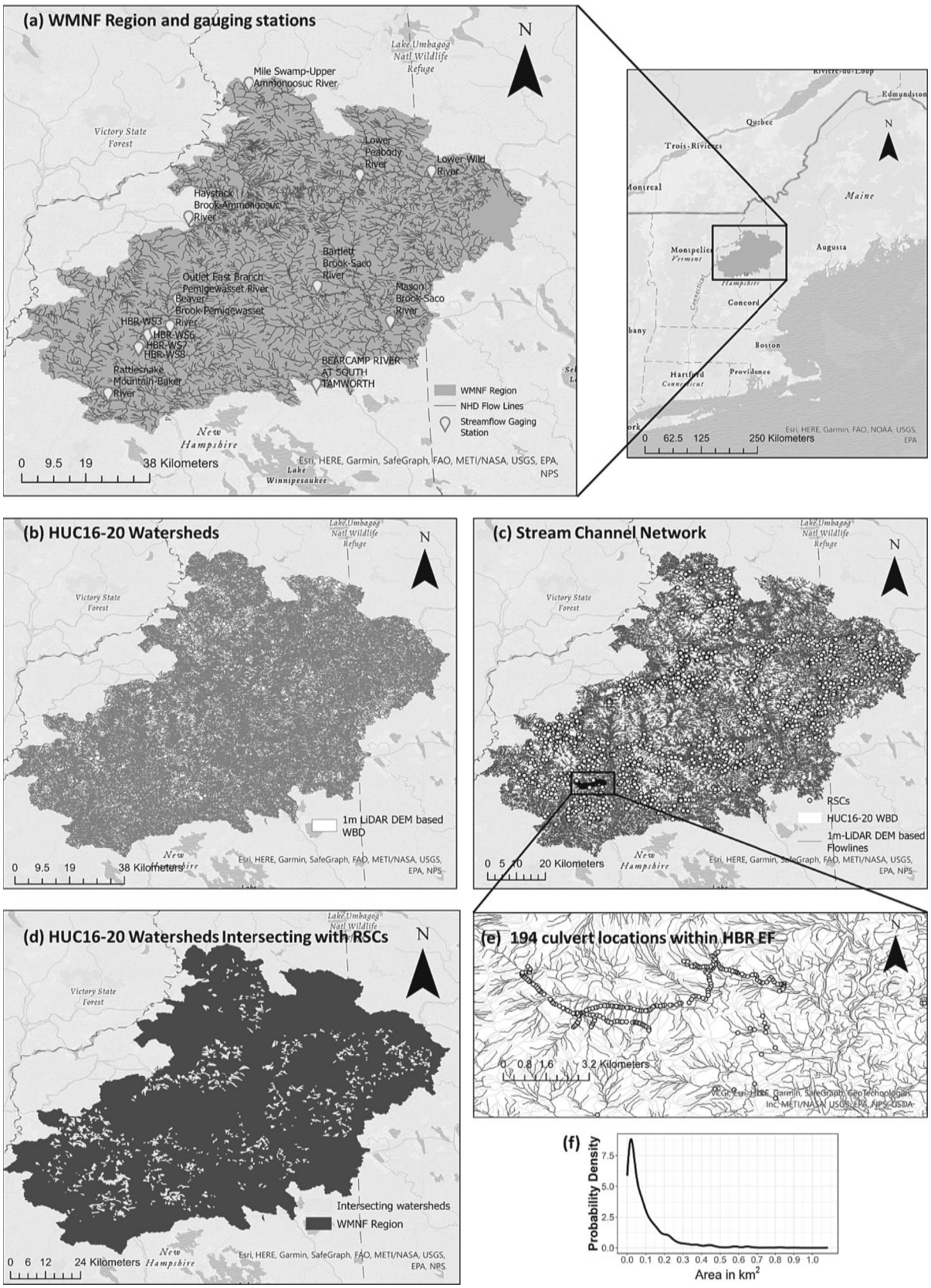

Fig. 2. Spatial maps showing the (a) WMNF region, major streams and rivers based on the national hydrography (NHD) dataset, and gauging stations (marked in yellow, refer to Table 2 for station ID) used in the study, (b) HUC16-20 watershed boundary (WBD) delineated based on the 1-m LiDAR DRM data, (c) 1-m LiDAR based stream network and 1,387 RSC and culvert locations (yellow circles) within the WMNF region, (d) 1,387 HUC16-20 watersheds intersecting that intersect with the RSC, and culverts (shown in c), (e) 194 culvert locations within the HBR EF, and (f) probability distribution of drainage area of the watersheds (all 14 gauged and 1387 ungauged watersheds). (For interpretation of the references to colour in this figure legend, the reader is referred to the web version of this article.)

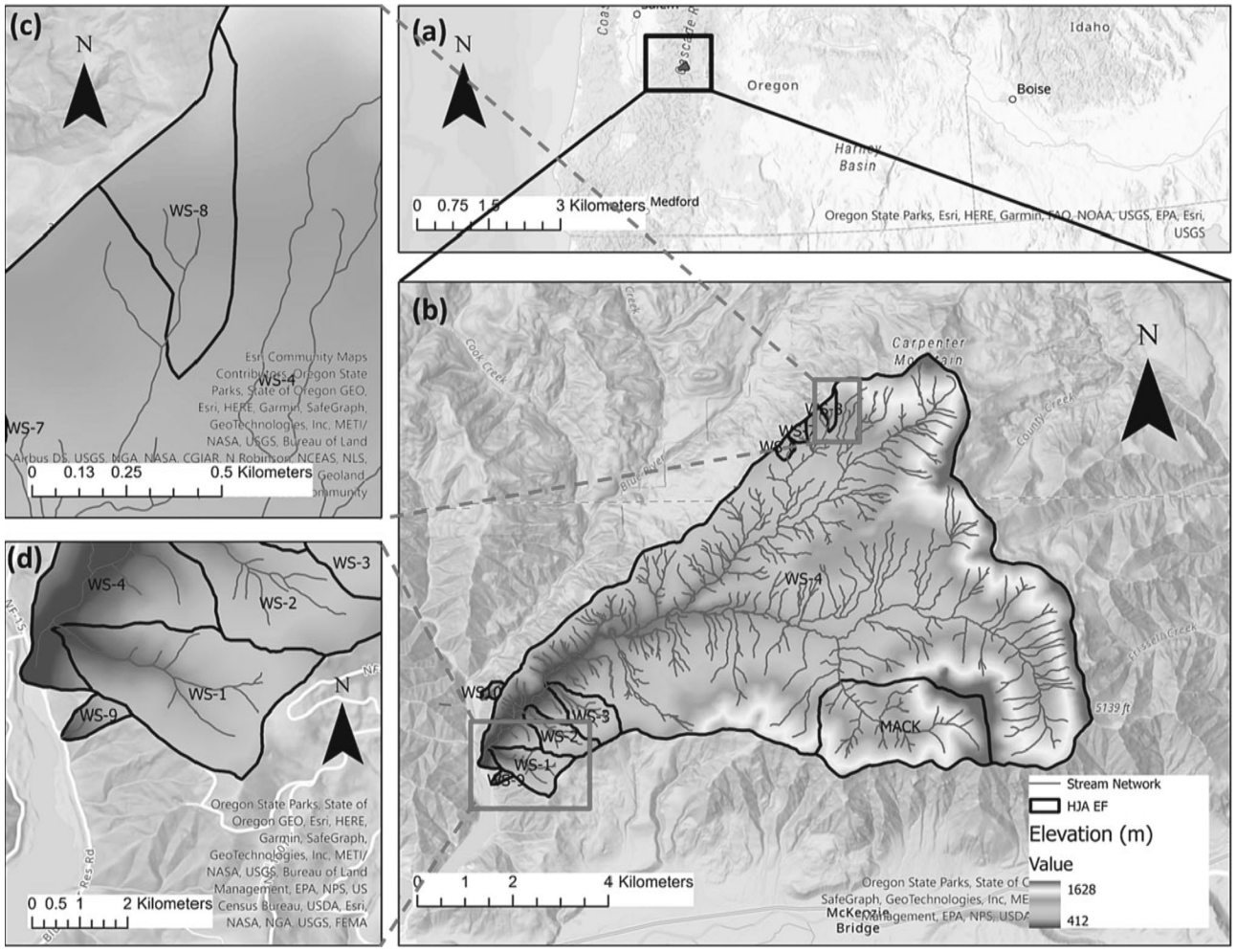

Fig. 3. Spatial maps showing (a) location of HJA EF, (b–d) the watershed boundaries, 10-m DEM elevation, and stream channels for the (b) HJA EF watersheds, (c) HJA-WS8, and (d) HJA-WS1 and HJA-WS9.

$$F_{GEV}(x|\mu,\sigma,\varepsilon) = exp\left[-\left(1+\frac{\varepsilon}{\sigma}(x-\mu)\right)^{-1/\varepsilon}\right], \mu \in R, \sigma > 0, \varepsilon \neq 0 \quad (2)$$

The *p*-quantile of the GEV distribution is then estimated as,

$$q_p = \left[\left(-\frac{1}{\ln(1-p)}\right)^{\varepsilon} - 1\right] \times \frac{\sigma}{\varepsilon} + \mu, (\varepsilon \neq 0) \quad (3)$$

where, (1-*p*) is the non-exceedance probability.

We used the same method outlined in Laio (2004) to conduct a goodness-of-fit (GOF) test. This method employs the Anderson-Darling (A-D) test statistics with reference to a composite hypothesis that a sample of observations comes from a distribution with unspecified parameters (at 5 % significance level; Laio, 2004). In this study, the GOF test is performed using the "*nsRFA*" R-package (Viglione et al., 2020).

By changing the model parameters, it is possible to incorporate the non-stationary climatic data in the GEV distribution (Eq. (3)) and capture the changes in the mean and variability within the distribution without changing the distribution's shape. This was accomplished by considering linear covariates in the μ, and σ parameter of the GEV model. In the analysis, ε parameter was kept constant, as it can be unrealistic to vary the ε parameter as a smooth function (Coles et al., 2001).

Given that significant trends in the AMS of peak discharges were detected based on the Mann-Kendall (M-K) trend test (Mann, 1945; Kendall, 1975) at 95 % confidence level, non-stationary information was included in the design discharge estimation by assuming antecedent soil moisture conditions (AMC) as a covariate in the location and scale parameter of the GEV distribution fit. Based on this assumption, the location and scale parameter were considered to vary linearly with AMC, leading to the choice of three competing GEV models, M0 (stationary), M1 (non-stationary in μ), and M2 (non-stationary in both μ, and σ; Table S1). Among these competing models, the best model was selected using the Akaike Information Criteria (AIC) and Likelihood Ratio Test (LRT; McCullagh and Nelder, 1989).

2.2.2. Regional parameter estimation

In the RFA, the site-specific parameters of the GEV distribution were calculated using the maximum likelihood estimation (MLE) methodology (El Adlouni et al., 2007). It is important to note that in the FA the site-specific parameters estimated with MLE were used to calculate the flood quantiles and their CIs. However, for the RFA, pooled growth curve estimates were computed after the at-site nonstationary parameter were estimated (O'Brien and Burn, 2014). To produce regional parameter estimates, at-site MLE based parameter estimations were first transformed into their corresponding L-moments of the GEV distribution using the transformation functions proposed by (Hosking, 1990). These L-moments were then integrated in accordance with Hosking and Wallis (1997):

$$\theta_k^R = \frac{\sum_{i=1}^{N} n_i \theta_k^{(i)}}{\sum_{i=1}^{N} n_i} \quad (4)$$

where, θ_k^R is the regional estimate of parameter *k*, *N* is the total number

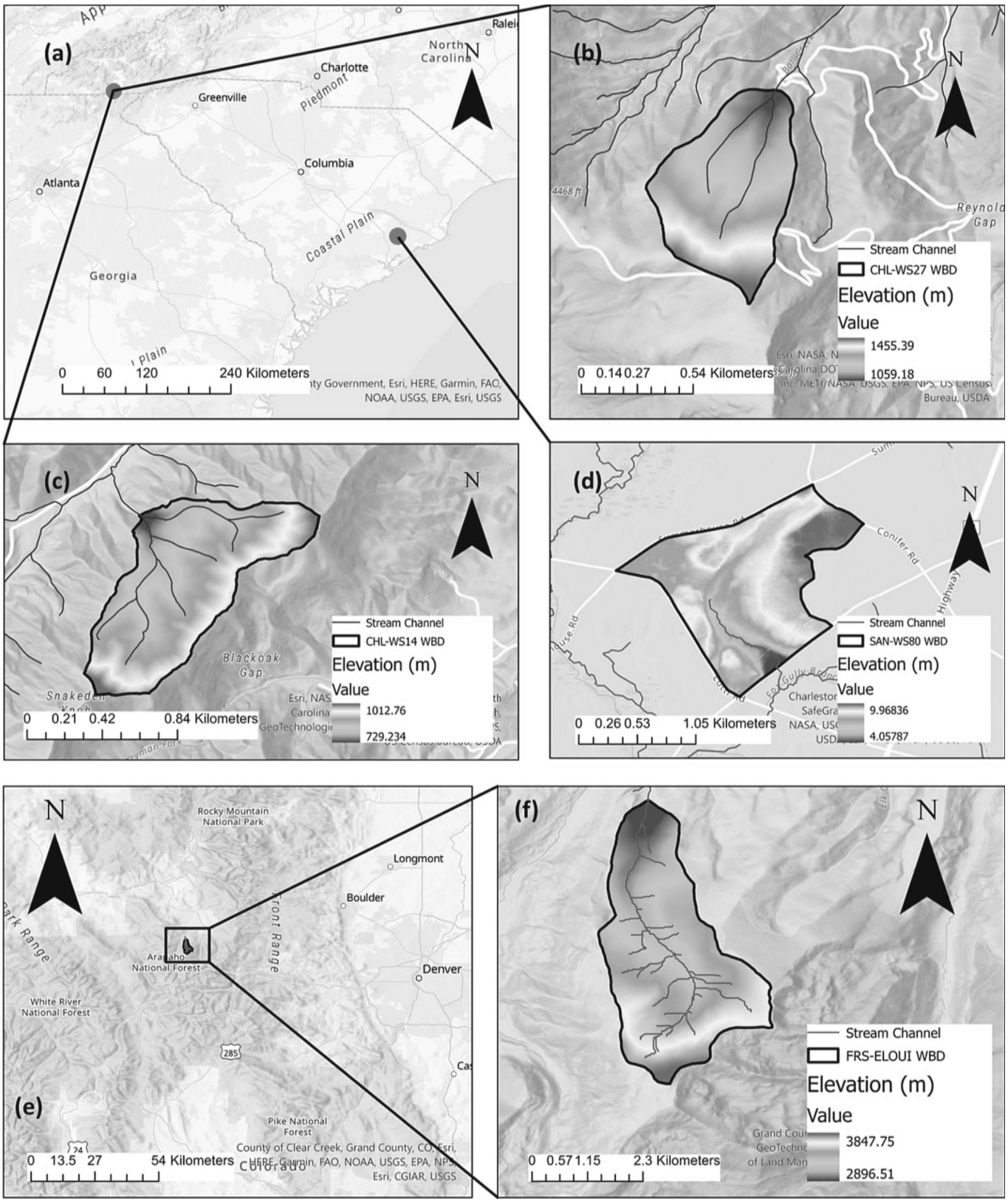

Fig. 4. Spatial maps showing the (a) location of CHL and SAN EF, (b–d) watershed boundary, 10 m DEM elevation, and stream channels for (b) CHL-WS14, (c) CHL-WS27, (d) SAN-WS80, and (e–d) same as in (a-d) but for FRS-ELOUI.

Table 2
Streamflow gauging stations and nearest rain gauges selected in the study for the WMNF and HBR region (within the WMNF region).

Site No.	Gauging Station-Streamflow Data								Nearest RG Station	
	Name of Gauging Station	Station ID	HUC16-20 WS ID	HUC16-20 WS Area (km^2)	HUC16-HCU20 WS Mean Elevation (m)	HUC16-HCU20 WS Slope (%)	HUC16-HCU20 WS Wetland Cover (%)	Data Period Used	RG Station ID	Distance (Km)
1	Bearcamp River at South Tamworth	USGS-01064801	USGS-01064801-d	0.4343	258.4	13.7	0.0	1993–2023	RG01	38.1
2	Rattlesnake Mountain-Baker River	USGS-01076000	USGS-01076000-d	0.0174	165.0	6.0	0.0	2001–2023	COOP:278885	13.2
3	Haystack Brook-Ammonoosuc River	USGS-01137500	USGS-01137501-d	0.016	367.1	6.3	0.0	1990–2023	COOP:276818	30.1
4	Lower Wild River	USGS-01054200	USGS-01054201-d	0.0074	226.9	14.6	0.0	1989–2023	COOP:276818	26.2
5	Lower Peabody River	USGS-01054114	USGS-01054114-d	0.086	252.8	7.0	0.0	2012–2023	COOP:276818	15.1
6	Mile Swamp-Upper Ammonoosuc River	USGS-01130000	USGS-01130000-d	0.0046	291.2	21.3	0.0	1991–2023	COOP:276234	11.2
7	HBR-WS7	HBR-WS7	HBR-WS7-d	0.1036	734.5	30.8	0.0	1965–2021	RG01	3.9
8	HBR-WS8	HBR-WS8	HBR-WS8-d	0.2524	826.5	20.8	0.1	1968–2021	RG01	4.8
9	HBR-WS6	HBR-WS6	HBR-WS6-d	0.1667	665.7	21.9	2.7	1963–2021	RG01	1.1
10	HBR-WS3	HBR-WS3	HBR-WS3-d	0.0911	670.9	19.8	0.0	1957–2021	RG01	1
11	Beaver Brook-Pemigewasset River	USGS-01075000	USGS-01075000-d	0.0573	199.4	5.5	0.0	2001–2023	RG01	4.6
12	Mason Brook-Saco River	USGS-01064500	USGS-01064500	0.0238	141.3	6.5	0.0	1987–2023	COOP:276818	32.5
13	Outlet East Branch Pemigewasset River	USGS-01074520	USGS-01074520-d	0.0169	262.1	13.7	32.6	1993–2023	RG01	11.8
14	Bartlett Brook-Saco River	USGS-010642505	USGS-010642505-d	0.0313	209.8	4.5	0.0	2009–2023	COOP:276818	19.5

of gauging stations in the region, n_i is the number of observations at the gauging station, i, and $\theta_k^{(i)}$ is the at-site estimate of parameter k. The transformation functions used in this study were originally proposed by Hosking (1990) and are summarized in the Supplementary Text S1. The calculated values of the site-specific L-moments of the GEV distribution (Hosking, 1990) were substituted to obtain the regional growth curve, $q(F)$. Finally, the regional growth curve function was substituted in Eq. (1) to calculate the site-specific quantiles for the specified return intervals (or exceedance probabilities). The confidence intervals (CIs) associated with the quantile estimates were defined by 95 % confidence level and calculated with Monte Carlo simulations (a 1,000 repeated samplings) using the "*lmomRFA*" R-package (Hosking, 2022). Hosking and Wallis (1997) provide a detailed discussion on the procedure followed for the estimation of the population parameters of the fitted distribution, regional and site-specific precipitation quantiles, and associated CIs.

2.2.3. Transferring information from gauged to ungauged watersheds

The design discharge estimates with the FA, RFA, and RM, from the gauged watersheds were mapped to the ungauged watersheds in accordance with the region of influence (ROI) criteria. The ROI was calculated based on the formation of clusters using 10 classification variables or parameters of the gauged and ungauged watersheds located within the WMNF and HBR EF boundary (Table 3). First the gauged sites that form a homogeneous region based on the watershed characteristics were identified using a cluster analysis followed by a heterogeneity test proposed by Hosking and Wallis (1997) and used in previous studies (Bonnin et al., 2006; Hosking and Wallis, 1997; Ngongondo et al., 2011; Srivastava et al., 2019). Finally, the ROI was formed by measuring the similarity between the homogeneous gauged, and ungauged watersheds based on the Euclidean distances in the space, defined by parameters of the gauged and ungauged watersheds, given by,

$$d_{ij} = \sqrt{\frac{1}{p}\sum_{h=1}^{p}\left(x_{hi} - x_{hj}\right)^2} \tag{5}$$

where, d_{ij} is the distance between two elements i and j given p different classification variables, and x_{hi} is the value of the h-th variable of the i-th element.

It should be noted that only three gauged watersheds among the 14 selected gauged watersheds in the WMNF region have wetland cover (Table 2). Therefore, to avoid information bias the wetland cover was not used as one of the watershed parameters for the identification of ROI in this study.

2.3. Rational method (RM)

The RM (Kuichling 1889) has been commonly used to estimate peak runoff rates in engineering projects in both urban and rural settings. The method has been applied in small watersheds (<80-ha or 200 acres) (Thompson, 2006) and in watersheds up to 260 ha (ODOT, 2014; Weaver and Hagans, 1994). The RM calculates peak flow rates based on the watershed area, precipitation intensity, and a runoff coefficient that indicates the proportion of precipitation that becomes runoff. The main assumptions of this method include (1) rainfall intensity is constant over the course of the storm, (2) rainfall distribution is uniform throughout the drainage area, (3) exceedance probability of peak discharge is same as that of precipitation intensity, (4) the drainage basin has no significant storage, and (5) the runoff coefficient is constant for a given watershed draining a culvert.

The RM can be formulated as,

$$Q = C_u CiA \tag{6}$$

where Q is the peak flow rate, C_u is the unit conversion coefficient, C is the runoff coefficient, or the percentage of precipitation converted to

Table 3
Classification variables or parameters of the gauged and ungauged watersheds used in the formation of region of influence.

Serial Number	Abbreviation	Description and source
1	LON, LAT	Coordinate of the centroid of watershed derived based on watershed delineation processed in Arc Hydro using the LiDAR based 1-m digital elevation model data.
2	TOPWET	Topographic wetness index, ln(a/S); where "ln" is the natural log, "a" is the upslope area per unit contour length and "S" is the slope at that point. (LiDAR based 1-m digital elevation model data)
3	HUC16-20 Longest Channel Length	Processed in Arc Hydro using LiDAR based 1-m digital elevation model data.
4	PRECIP	Mean annual precipitation from the PRISM dataset for 1991–2020
5	ELEV	Mean watershed elevation (meters) from LiDAR based 1-m digital elevation model data.
6	SLOPE	Average Slope (%) of the watershed derived from LiDAR based 1-m digital elevation model data.
7	AREA	Watershed drainage area, km^2
8	HSOIL	Hydrological Soil group obtained from Oak Ridge National Laboratory Distributed Active Archive Center.
9	CN	Average curve number of a watershed derived from the Hydrological Soil group dataset.
10	TcNRCS	Time of concentration derived using the NRCS lag-time method.

runoff, i is the design rainfall intensity based on the watershed time of concentration (Tc), and A is the watershed drainage area. Tc was calculated with the NRCS time-lag method that uses the longest stream channel length and average curve number of a small or medium sized watershed (Folmar et al., 2007). As we were interested in the peak discharge response to extreme storm events, the mean C value was generated by back-calculation for any given gauged watershed by applying the RM to the top 1000 extreme storm events with their PIs (based on the Tc) and their corresponding instantaneous peak discharges. The mean C value was further adjusted by factors of 1.1, 1.2, and 1.25 for return intervals of 25, 50, and 100 years, respectively, as used in Hayes and Young (2006) and advised by ODOT (2014) to design for extremely rare flood events. The Supplemental Material Text S2 and S3 include a thorough explanation of how Tc and C were derived in this study.

2.4. USGS regional regression equation (RRE)

The USGS RREs are generated with generalized least squares regression based on regionalized flood frequency data for a collection of gauged stations within a hydrologically homogeneous region. These predictive equations are frequently used to estimate design discharge at various return intervals and illustrate the statistical link between flood frequency analysis-based estimations and basin variables (e.g., basin area, impervious percentage, slope, maximum rainfall intensity, etc.) (Table S2). Following Amatya et al. (2021a–c), we used the equations reported by Weaver et al. (2009) for the CHL EF rather than the most recent Feaster et al. (2014) equations because the later did not include equations for region 2 (Blue Ridge ecoregion) in North Carolina, where the CHL is located.

2.5. Evaluation of the design discharges

In this study, percentage bias (PB; Mizukami et al., 2019) was calculated to evaluate how well Q_p estimates from the deterministic and semi-empirical methods like the RM, and statistical methods like the USGS RRE agreed with the probability based Q_p estimates derived from observed streamflow records. PB is calculated as,

$$PB = \frac{(Q_o - Q_E)}{Q_o} \times 100 \tag{7}$$

where:

Q_0 – design discharge, calculated using the probability-based frequency analysis.

Q_E – design discharge, calculated using the deterministic methods, such as, the RM, and USGS RREs.

2.6. Hydrologic vulnerability assessment for road culverts

Hydrologic vulnerability of the road culverts in this study was assessed based on the ability of the culvert to accommodate the design discharge of interest without a failure due to overtopping. This was achieved by comparing the Q_c of a culvert draining a specific watershed with the design peak discharge estimate for that watershed at its outlet. The Q_c is defined as the allowable passage flow rate through a culvert and was calculated using the orifice flow equation assuming a submerged inlet control. Mathematically, the orifice flow equation (Malcom, 1989) gives the mass flow rate (or Q_c) through an orifice, given the area of the orifice, A, and can be written as:

$$Q_c = C_d \times A \times \sqrt{2gH} \tag{8}$$

where C_d is the coefficient of discharge, g is the acceleration due to the gravity of Earth (in m/s^2), and H is the driving head or the mean center line (the distance between the water surface level and the centroid of the culvert, in m). The C_d, a dimensionless coefficient of discharge, is equal to 0.62 for a square-edged entrance and when the flow approaches a well-rounded entrance with a submerged inlet (bank-full) condition (Franzini and Finnemore, 1997). While ASCE (1992) suggests equation (8) is applicable only when $H/D \geq 2$, Franzini and Finnemore (1997) established that the error is only 2 % when $H/D \geq 1.2$, where D is the diameter of the culvert. In this study, we based our calculations on the later assumption that $H \approx 1.2D$.

For a given return interval or exceedance probability of a design discharge, a culvert is deemed hydrologically vulnerable if the design discharge for the watershed is greater than either the bank full discharge or the magnitude of Q_c, representing the culvert capacity. However, it was beyond the scope of this study to quantify the probability of failure risk of these vulnerable culverts by accounting for the exceedance of design discharge over their life span used in cost-benefit analyses (Hansen, 1987).

3. Results and discussion

3.1. Comparison of peak design discharge estimates and uncertainties for the WMNF region

The magnitude of the annual peaks of 15-min instantaneous streamflow discharges per unit drainage area and their linear trends for the 14 gauging stations selected within and adjacent to the WMNF, and HBREF are shown in Fig. S1. Out of the 14 gauging stations, the annual peak discharges per unit drainage area for the three gauging stations in HBR, HBR-WS3, HBR-WS6, and HBR-WS7 were found to exhibit statistically significant (at 95 % confidence level) increasing trends based on the Mann Kendall (MK) Trend test (Fig. S1, Table 2; Mann, 1945; Kendall, 1975). The results of the GOF test, used for assessing the suitability

of the extreme value distribution used in the analysis are summarized in Table 4. The GOF test indicated that the GEV distribution shows a statistically good fit at 95 % confidence level for all gauging stations, except for one gauging station for which the Gumbel distribution is indicated as a statistically good fit.

Numerous studies (Eisenbies et al., 2007; Beier et al., 2015; Fang and Pomeroy, 2016; Cea and Fraga, 2018) have highlighted increase in the AMC is linked to significantly increasing trends in streamflow discharges leading to more severe floods in hydrologic systems, such as in the HBR EF. This is particularly important in the context of changing climate and the increased frequency of precipitation extremes that have led to extended periods of saturated soil conditions that contribute to floodings (Eisenbies et al., 2007; Mukherjee et al., 2023), and landslides in some cases (Ward et al., 2020; Kirschbaum et al., 2020). The Pearson correlation analysis suggests a statistically significant (at 95 % confidence level) relationship between AMC and the annual peak discharges per unit drainage area at the HBR-WS3, HBR-WS6, and HBR-WS8 gauging stations as shown in Fig. S2. AMC was calculated as the 5-day sum of 24-hr precipitation (obtained from the nearest rain gauge station, Table 2) prior to the day of the peak discharge event. Subsequently, non-stationary GEV modeling assumptions were applied for these three gauging stations with the AMC as a covariate, which were further evaluated to determine the best fit GEV model using the AIC and LRT test criteria as shown in Table S3. Table S4 illustrates the GEV parameters estimated with MLE, their transformed L-moments and L-moment ratio (see Text S1 for Methods), and estimated index flood magnitude used in the RFA for the gauged watersheds.

The 25-yr, 50-yr, and 100-yr Q_p estimated by the RM and USGS-RRE were focused on the HUC16-20 watersheds corresponding to the 14 gauging stations at the WMNF and HBR EF. Tables S5 and S6 list the variables and their values used in the calculation of the peak discharges with the RM and USGS-RRE (see Methods). The *Tc* was found to vary from 7-mins to 3-hr for the gauged HUC16-20 watersheds (Table S5).

The magnitudes of Q_p (and uncertainties) for 25-yr, 50-yr, and 100-yr return periods, calculated using the three selected methods, the stationary or non-stationary RFA, RM, and USGS-RRE for the selected gauging stations, are shown in Fig. 5(a–c) and Tables S7–S9. The agreements among these three methods were evaluated based on the PB statistics (see Methods), as shown in Fig. 5(d–f) and Table S10. The Q_p magnitudes, calculated using the RFA, are comparable with the magnitudes of observed annual peak discharges at all the gauging stations, particularly for HBR-WS8. This comparability is also noteworthy at HBR-WS7, where non-stationarity was detected in the mean as well as in the variability of the distribution of annual peak discharges (Table S3). Consequently, the 25-yr, 50-yr, and 100-yr Q_p magnitudes at this gauging station were greater than the other gauging stations, HBR-WS3, and HBR-WS6. Importantly, HBR-WS7-d, and HBR-WS8-d are north-facing watersheds which naturally get more precipitation along with lower evapotranspiration, potentially resulting in higher AMC than other watersheds within the HBR EF (Campbell et al., 2011). This is reflected in the Q_p magnitudes estimated by the RFA for HBR-WS7-d, and HBR-WS8-d which was greater than the values estimated for the rest of the watersheds.

Furthermore, for most of the gauged watersheds, the 25-yr, 50-yr and 100-yr Q_p values estimated by the RFA agree well with those estimated by RM and the USGS-RRE. This is indicated by the magnitude of estimated PB which fell within the range of 0–50 % for most of the gauges. However, there was considerable disagreement among methods in some cases, especially the watersheds, USGS-01064801-d, USGS-01076000-d, USGS-01130000-d, USGS-01137500-d, and USGS-01064500-d. Among these gauging stations, the PB in the peak discharge estimates for the watersheds USGS-01076000-d, USGS-01137500-d, USGS-01130000-d, USGS-01064500-d suggest that the RM method overpredicts the 25-yr, 50-yr, and 100-yr Q_p estimates by 296–306 %, 99–111 %, 406–440 %, 102–115 %, respectively, as compared to those estimated by the RFA. On the other hand, the USGS-RRE method overpredicts the 25-yr, 50-yr, and 100-yr Q_p estimates for USGS-01064801-d, USGS-01130000-d, and USGS-01064500-d watersheds by 254–293 %, 394–485 %, and 319–405 %, respectively, as compared to those estimated by the RFA. The considerably large and unidentified uncertainty in Q_p could come from extrapolating the prediction equations to smaller watersheds outside the boundaries of the regression data used to develop the USGS-RRE (Genereux, 2003).

Fig. S3 illustrates the ROI of the HUC16-20 gauged watersheds across the ungauged watersheds that intersect with the RSCS within the WMNF and HBR region. The 25-yr, 50-yr and 100-yr Q_p values for the ungauged HUC16-20 watersheds are shown in Fig. S4, Fig. S5, and Fig. 6, respectively. The Q_p estimated by the RFA and RM method show a better agreement for almost all the watersheds as compared to the USGS-RREs, although the RM slightly underpredicts the Q_p in both gauged and ungauged watersheds. This is indicated by the lower magnitude of PB values for the ungauged watersheds (Fig. 6d) which are mostly within a range of 0 % to 50 % for Q_p estimated by the RM. In contrast, the USGS-RREs overpredicts the Q_p by 25–50 % for most of the watersheds, as indicated by the magnitude of PB in Fig. 6e. Interestingly, USGS-RREs use percentage of wetland area as one of the key variables for Q_p estimation for streams in New Hampshire. Results indicate that the USGS-RREs yielded considerably greater Q_p estimates and a higher overprediction (greater PB) for the study watersheds with fewer wetland areas as compared to the watersheds with larger wetland areas, as demonstrated in Fig. S6. A significantly strong negative relationship between the Q_p and proportion of wetland area of the ungauged watersheds (Pearson Correlation coefficient, $R = -0.6$; p-value < 0.05) can be seen in Fig. S6 (f). The greater storage provided by wetlands and floodplain in the watershed attenuates the peak discharge in the channel (Amatya et al., 2019), which may have ultimately impacted the Q_p

Table 4
Results of trend analysis based on Mann Kendal (MK) trend test (at 5% significance level), and Goodness-of-fit (GOF) test using the Anderson-Darling (AD) Statistics for the gauged HUC16-20 watersheds in the WMNF region.

Serial Number	HUC16-20 WS-ID	Number of years analysed	MK Trend Test (p-value)	Selected Distribution Fit	AD Statistics	AD Test (p-value)
1	USGS-01064801-d	31	0.103	GEV	0.189	0.140
2	USGS-01076000-d	23	0.712	GEV	0.408	0.819
3	USGS-01137500-d	34	0.847	GEV	0.205	0.220
4	USGS-01054200-d	35	0.989	GEV	0.224	0.303
5	USGS-01054114-d	12	0.945	GEV	0.195	0.206
6	USGS-01130000-d	29	0.420	GEV	0.307	0.604
7	HBR-WS7-d	57	0.013	GEV	0.393	0.785
8	HBR-WS8-d	54	0.199	GEV	0.170	0.115
9	HBR-WS6-d	59	0.030	GEV	0.242	0.361
10	HBR-WS3-d	65	0.002	GEV	0.206	0.227
11	USGS-01075000-d	23	0.812	Gumbel	0.630	0.899
12	USGS-01064500-d	37	0.855	GEV	0.264	0.453
13	USGS-01074520-d	31	0.434	GEV	0.434	0.852
14	USGS-010642505-d	15	0.656	GEV	0.475	0.899

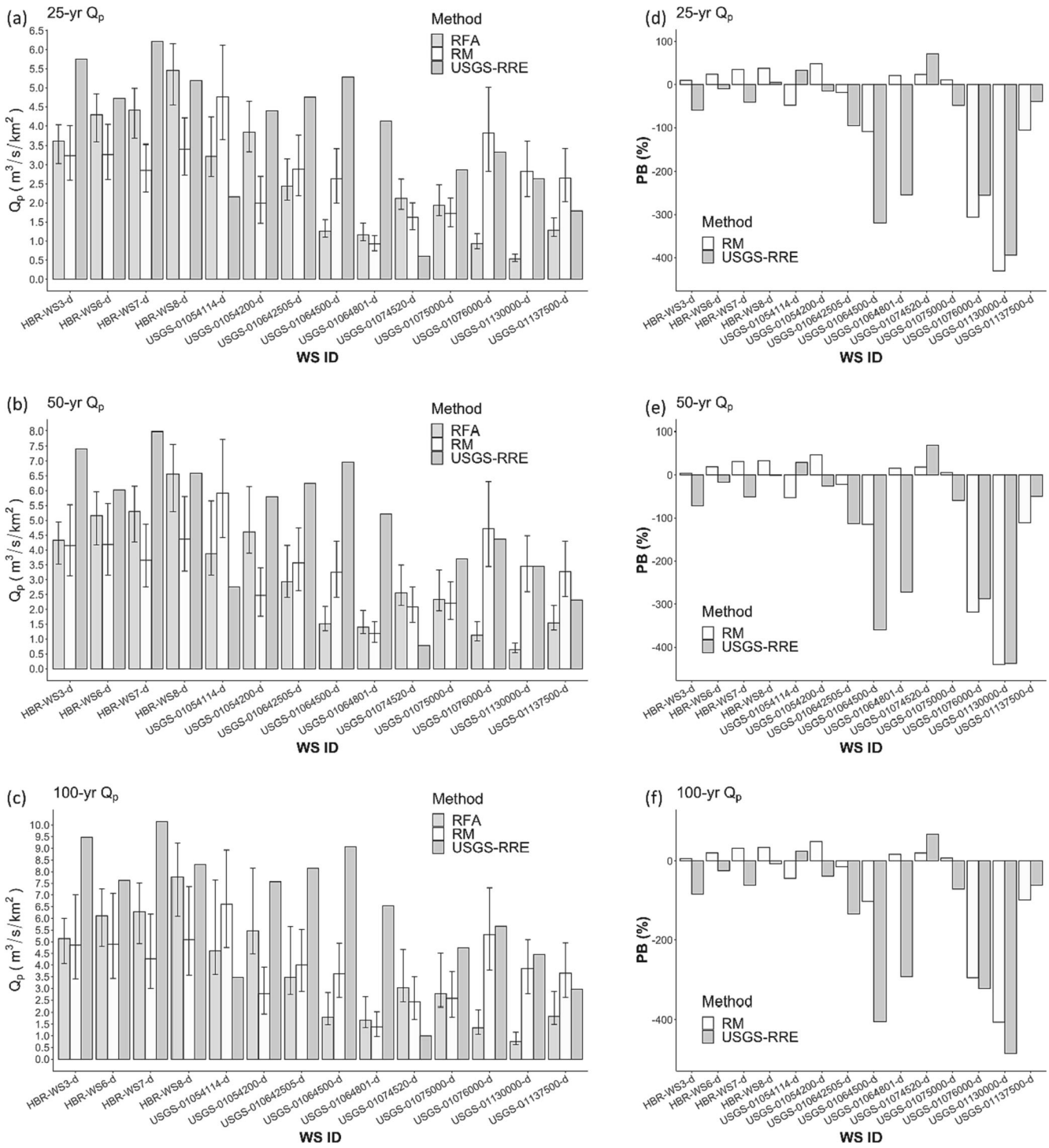

Fig. 5. Comparison of (a) 25-yr, (b) 50-yr, and (c) 100-yr Q_p (shown by bar) and 5–95% confidence intervals (shown by error bars) for HUC16-20 gauged watersheds (shown by WS ID) selected within and adjacent to the WMNF (and HBR EF) region estimated by the RFA, RM, and USGS-RRE methodology. The corresponding PB (%) for the 25-yr, 50-yr and 100-yr peak discharge are shown in (d–f) for the RM and USGS-RRE methodology. It is important to note that for the RFA analysis, non-stationary model was selected as the best fit model for the gauged watersheds, HBR-WS3-d, HBR-WS6-d, and HBR-WS7-d, and stationary model was selected as the best fit for the rest of the watersheds (refer to Table S3).

estimates.

The RM performed well in small watersheds with drainage area of less than the 120-ha limit recommended for the method in the literature (Thompson, 2006; ODOT, 2014). All the study watersheds are at a scale of HUC16-20 with a drainage area of less than 50-ha, whereas the USGS equations were derived using data from watersheds with a drainage area greater than 180-ha (Olson, 2008). This raises questions about the reliability of using the USGS-RREs as compared to the RM for estimating Q_p estimates for these small watersheds. One possible explanation for the better performance of RM in small watersheds is that the RM assumes negligible water storage and, accordingly, the flood estimates respond linearly to increases in PI (Amatya et al., 2021a–c) unlike the USGS-RREs that were developed assuming a linear connection between flood estimates and the drainage area of the watersheds. This also

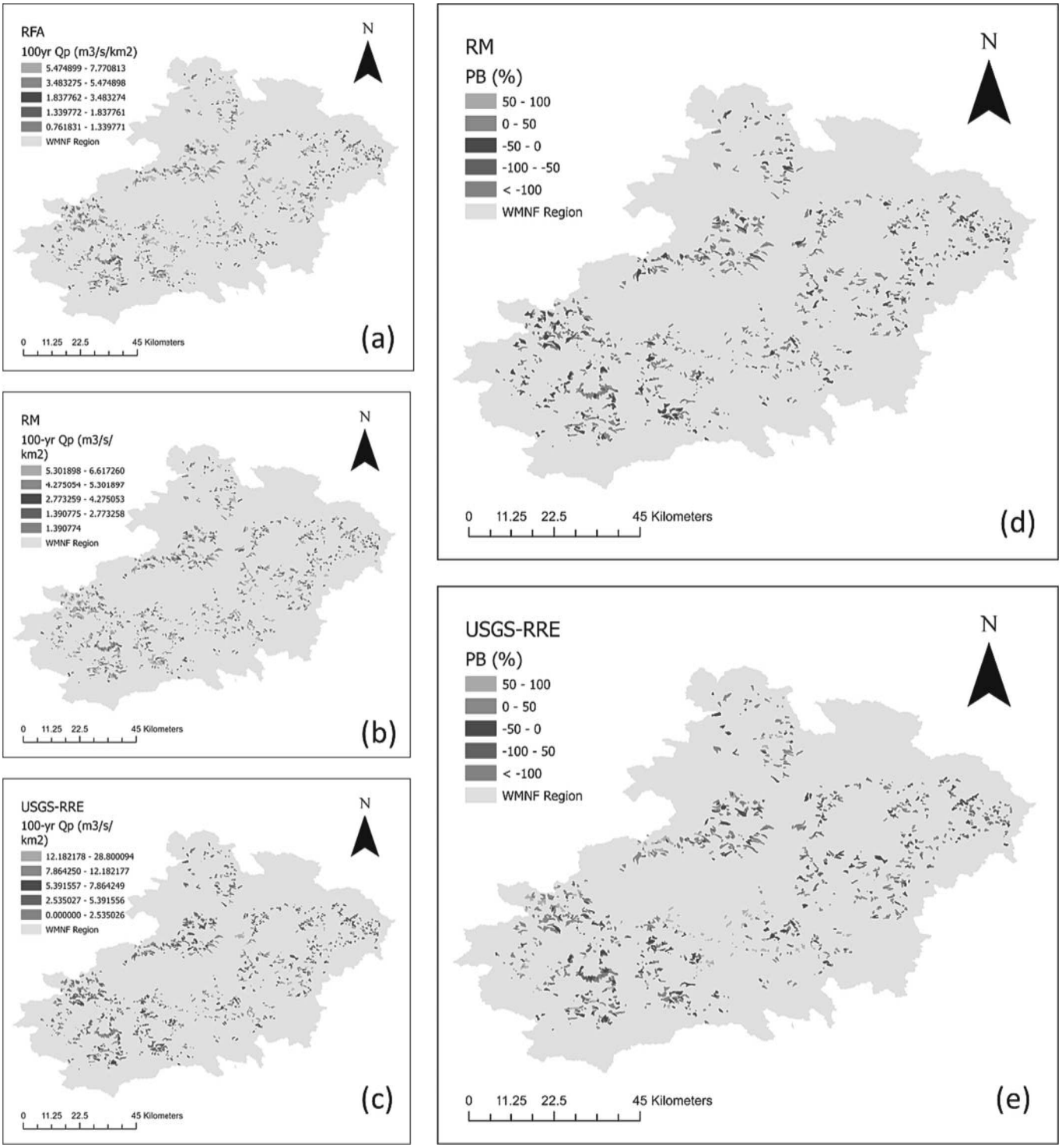

Fig. 6. Spatial map showing the (a–c) 100-yr Q_p (in $m^3/s/km^2$) estimated by the (a) RFA, (b) RM, and (c) USGS-RRE methodology, and (d–e) the PB (in %) for the 100-yr Q_p estimated by (d) RM and (e) USGS-RRE methodology compared to RFA for the HUC16-20 (gauged and ungauged) watersheds within the WMNF that intersects with the culverts and RSCS.

explains why the PB for the Q_p estimated by RM is greater for the higher RI, while PB for the Q_p estimated with the USGS-RRE is independent of the increase in RI (Fig. 5(d–f), and Fig. 6(d–e)).

3.2. Comparison of peak design discharge estimates for other study watersheds

Fig. S7 depicts the magnitude of the yearly peaks of 15-min instantaneous discharge per unit drainage area and associated linear trends for the seven gauging stations for the reference watersheds, two within the CHL (WS ID: CHL-WS14, and CHL-WS27), one within the FRS (WS ID: FRS-ELOUI), three within the HJA (HJA-WS1, HJA-WS8, and HJA-WS9), and one within the SAN (WS ID: SAN-WS80). Given that 15-min instantaneous streamflow data was available for more than two reference watersheds only within the HJA, we performed the RFA for the gauging stations located within that HJA EF, whereas single-site

frequency analysis (FA) was performed for study watersheds in all other EFs.

A storm on October 3–4, 2015, influenced by Hurricane Joaquin caused nearly 500 mm rainfall within 48-hr in South Carolina. This storm potentially raised the annual peak discharge measured at the SAN-WS80 gauging station for the year 2015 (St. George and Mudelsee, 2019) as shown in Fig. S7, causing high non-linearity and artifact in the annual variability of the flood peaks over the selected period. Therefore, an additional analysis was also performed for SAN-WS80 by removing the year 2015 peak discharge, hereafter denoted as SAN-WS80R.

For CHL-WS14 and CHL-WS27 watersheds, the Gumbel method was selected as the best fitted distribution as per the GOF test based on AD statistics (Table 5). For all other EF watersheds, the GEV distribution was selected as the best fitted distribution. The yearly peak discharge for the HJA-WS1 gauging stations, was found to have a statistically significant (at 95 % confidence level) increasing trend, as determined by the M-K Trend test (Fig. S7, Table 5; Mann, 1945; Kendall, 1975). As such, non-stationary GEV modeling assumptions were applied for this gauging station with AMC as covariate, which was further evaluated to determine the best fit GEV model using the AIC and LRT test criteria as indicated in Table S11. Table S12 illustrates the transformed L-moments, L-moment ratio (see Text S1 for Methods), and estimated index flood magnitudes used in the RFA for the HJA's study watersheds. Table S13 illustrates the 25-yr, 50-yr, and 100-yr Q_p values estimated with MLE for both RFA and FA for all the EFs.

Large disparities between the Q_p determined by the RM using on-site PIs and the USGS-RRE are evident in Fig. 7 and Tables S13–S16. In CHL watersheds, both the RM and USGS-RRE overpredict the Q_p estimates compared to the FA. However, the RM performed better than the USGS-RRE which can be attributed to the smaller size of the watersheds (CHL-WS14: 61-ha, and CHL-WS27: 39-ha) where the assumptions of uniform rainfall and negligible storage hold. Furthermore, measurements from rural watersheds larger than 260 km^2 area were used to create the USGS-RRE for the Blue Ridge region of North Carolina, where the CHL-WS14 and CHL-WS27 watersheds, with substantially smaller drainage area, are located (Weaver et al., 2009). The USGS-RRE substantially overpredicted the Q_p estimates for CHL-WS14 which is a relatively larger watershed compared to CHL-WS27. In contrast, the Q_p estimated by the RM is greater for the smaller watershed, CHL-WS27, with overprediction of the Q_p by as much as 88–124 % compared to the RFA using the observed streamflow records. However, large uncertainty in Q_p can be noted for the RM method which may stem from the large uncertainty of onsite design storm PI at the CHL-RG31 (Table 1; Mukherjee et al., 2023). These findings are consistent with previous studies on the same forested watersheds (Genereux, 2003, Amatya et al., 2021a–c). For example, Genereux (2003) suggested that the RM, based on a 50-year Q_p estimate, outperformed other methods such as the USGS RRE, the NRCS TR-55 method, and the North Carolina Department of Transportation methods for a 19.6-ha 66 % forested watershed in North Carolina's Piedmont region.

Interestingly, both the RM and USGS-RRE performed well at FRS-ELOUI watershed with RM and USGS-RRE underpredicting the 100-yr Q_p by 61 %, and 46 %, respectively compared to the FA (Fig. 7, Table S16). Although the drainage area of the watershed is considerably large (259-ha) for the assumptions of the RM to hold, the high gradient (average slope of 72.4 %) mountainous streams likely overcome the prediction error associated with minimal storage assumption of the RM (David, 2011) that has been identified to be a source of prediction error for low-gradient, 160-ha watershed with substantial storage (Amatya et al., 2021a–c).

At the HJA there was a strong relationship between flood estimates and drainage area. For example, RM performed well compared to RFA for the small watershed, HJA-WS8 (20.4-ha), underpredicting 25-yr, 50-yr, and 100-yr Q_p by 11 %, 4 % and 0 %, respectively. PB associated with the RM was relatively greater for HJA-WS1 (95.9-ha or 0.959 km^2), overpredicting the 25-yr, 50-yr, and 100-yr Q_p by 43 %, 39 %, and 37 %, respectively. Both USGS-RRE and RM performed poorly in predicting the 100-yr Q_p for the very small watershed, HJA-WS9 (8.5-ha), overpredicting Q_p by 287 %, and 377 %, respectively.

In SAN-WS80, the RM underestimated the design discharge by up to 61 % for a return interval greater than 25-years. On the other hand, the USGS-RRE underestimated it by just 8 %. This is in agreement with Amatya et al. (2021a–c) which found similar large underestimation by RM and somewhat overprediction by the USGS-RRE at that time when streamflow data, available only through 2016, was used. In addition, both FA and RM showed large uncertainties in their Q_p estimates. The large uncertainties in Q_p estimated by FA can be attributed to the statistical artifact imposed by the non-linearity in the variation of annual peak streamflow records at the SAN-WS80 gauging station caused by the indirect influence of the 2015 Hurricane Joaquin in South Carolina. Interestingly, the uncertainty associated with the Q_p at this site significantly reduced after removing the flow event associated with this 2015 extreme event as shown in Fig. 7 for the site ID SAN-WS80R. The large uncertainties in Q_p estimated by the RM, however, is most likely because it is gently sloped watershed with significant storage (Amatya et al., 2021a–c) and a large drainage area (160-ha), which exceeds the 120-ha limit specified for the approach (Thompson, 2006; ODOT, 2014; Amatya et al., 2021a–c). Overall, these findings indicate that the RM works better for smaller watersheds (WS14 and WS27 in NC, and HJA-WS8 in OR) with drainage area up to 120-ha, whereas the USGS RRE is more reliable for larger watersheds (SAN-WS80, FRS-ELOUI) at flood return intervals (>=25-yr), normally of importance for design/sizing of RSCS and culverts.

However, it is important to note that with the RM there is a lack of consideration for any storage features, such as wetlands, channels, and floodplains, that do not entirely fill and reach a continuous inflow-outflow state during a storm event (ODOT, 2014). This omission can be an important source of error in deriving Q_p on the watersheds with considerable portion of wetland area within the WMNF region and may be supplemented by the uncertainties associated with the estimation of the runoff coefficient stemming from uncertainties in PIs (Grimaldi and Petroselli, 2015a,b; Tedela et al., 2012). Accumulated snow cover in snow-dominated watersheds in the HJA, HBR, and FRS EF can also lead to greater magnitudes and uncertainties of the runoff coefficient (Merz and Blöschl, 2009). Previous research has shown that combining runoff coefficients and *Tc* obtained from field measurements, where possible

Table 5
Results of trend analysis based on Mann Kendal (MK) trend test (at 5% significance level), and Goodness-of-fit (GOF) test using the Anderson-Darling (AD) Statistics for the study watersheds located in CHL-, FRS-, HJA-, and SAN-EF.

Gaging Station /WS ID	Number of years analyzed	MK Test (p-value)	Distribution	AD Statistics	AD test (p-value)	Type of Analysis Performed
CHL-WS14	39	0.61	Gumbel	0.66	0.91	FA
CHL-WS27	40	0.27	Gumbel	0.60	0.88	FA
FRS-ELOUI	78	0.66	GEV	0.27	0.39	FA
HJA-WS1	67	0.02	GEV	0.48	0.86	RFA
HJA-WS8	56	0.90	GEV	0.29	0.54	RFA
HJA-WS9	51	0.17	GEV	0.39	0.75	RFA
SAN-WS80R	40	0.77	GEV	0.36	0.73	FA
SAN-WS80	41	0.99	GEV	0.37	0.74	FA

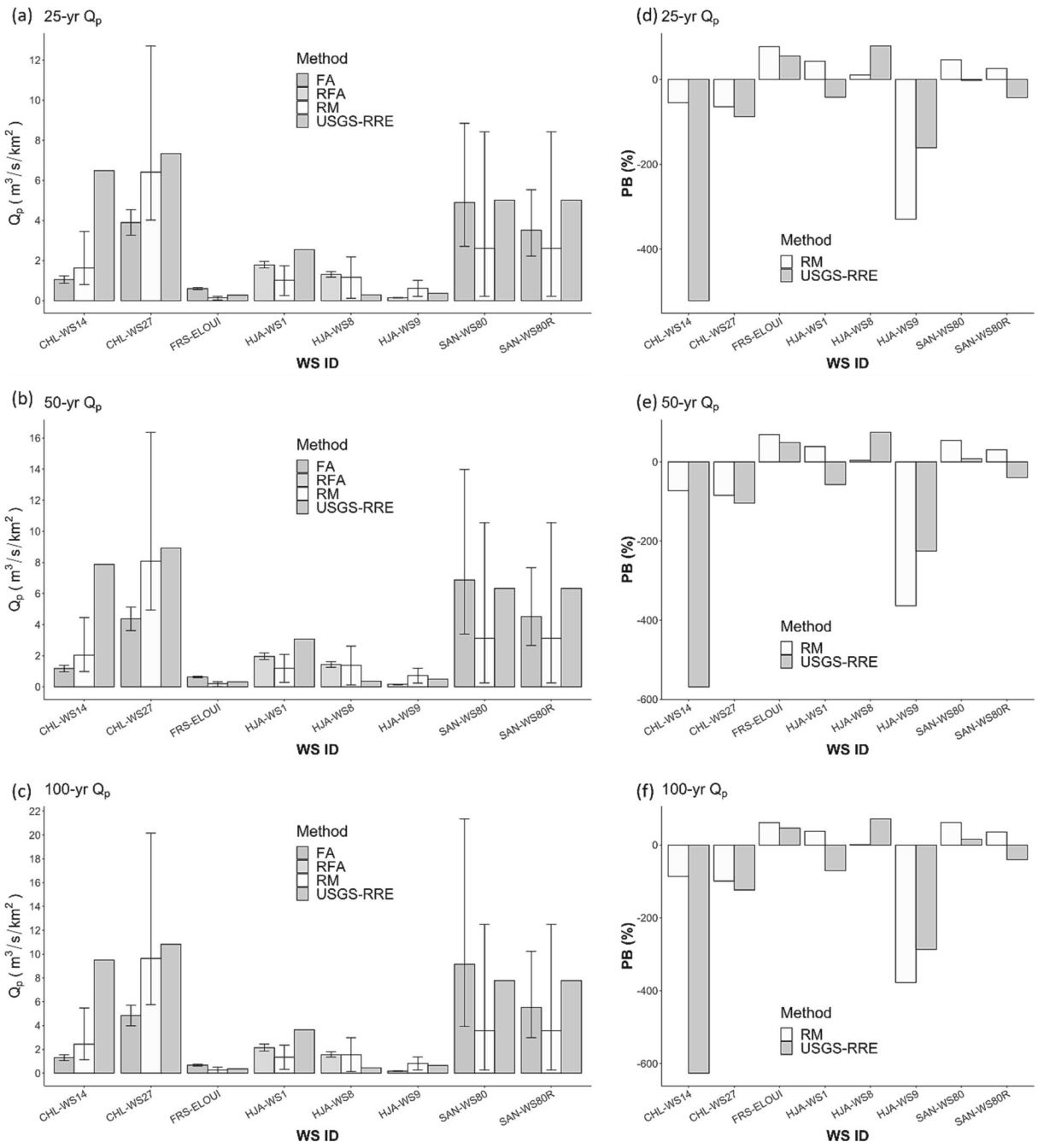

Fig. 7. Comparison of (a) 25-yr, (b) 50-yr, and (c) 100-yr Q_p (shown by bar) and 5–95% confidence intervals (shown by error bars) for HJA, CHL, SAN, and FRS EF watersheds estimated by the RFA, FA, RM, and USGS-RRE methods. The corresponding PB values for the 25-yr, 50-yr and 100-yr peak discharge are shown in (d–f) for the RM and USGS-RRE methodology. It is important to note that for the RFA analysis, non-stationary model was selected as the best fit model for the gauged watershed, HJA-WS1, and stationary model was selected as the best fit for the rest of the watersheds (refer to Table S11).

(Hayes and Young, 2006; Thompson, 2006; Trommer et al., 1996) and varied return intervals (McEnroe et al., 2013), can greatly enhance RM estimations.

3.3. Hydrologic vulnerability of culverts within the HBR

Hydrologic vulnerability assessment of road culverts was performed only for the HBR EF region using a dataset of total 194 culverts. The culvert diameters (D) ranged from 0.38 m (15 in) to 1.83 m (72 in), as shown in Fig. 8a. Fig. 8b illustrates the estimated hydraulic capacity of each of these culverts (see Methods for estimation of hydraulic capacity). Out of the 194 culverts, 140 culverts have a diameter of 0.46 m (18 in). The minimum and maximum hydraulic capacity across these culverts with different sizes vary between 0.2 $m^3\ s^{-1}$ (for D = 0.38 m) and 10.7 $m^3\ s^{-1}$ (for D = 1.83 m).

Fig. S8, Fig. S9, and Fig. 8(c-d) illustrate the hydrologic vulnerability of the 194 culverts to various levels of flood discharge, i.e., for 25-yr, 50-yr, and 100-yr flood return periods, respectively, estimated by the RFA, RM, and USGS-RRE. The culverts with Q_c greater than the flood design discharge (Q_p x watershed drainage area) magnitude with a return period of interest are determined as adequately sized for that flood return period, as shown by yellow circles. On the other hand, the culverts failing to accommodate the passage of the flood design discharge magnitude with a return period of interest are determined to be

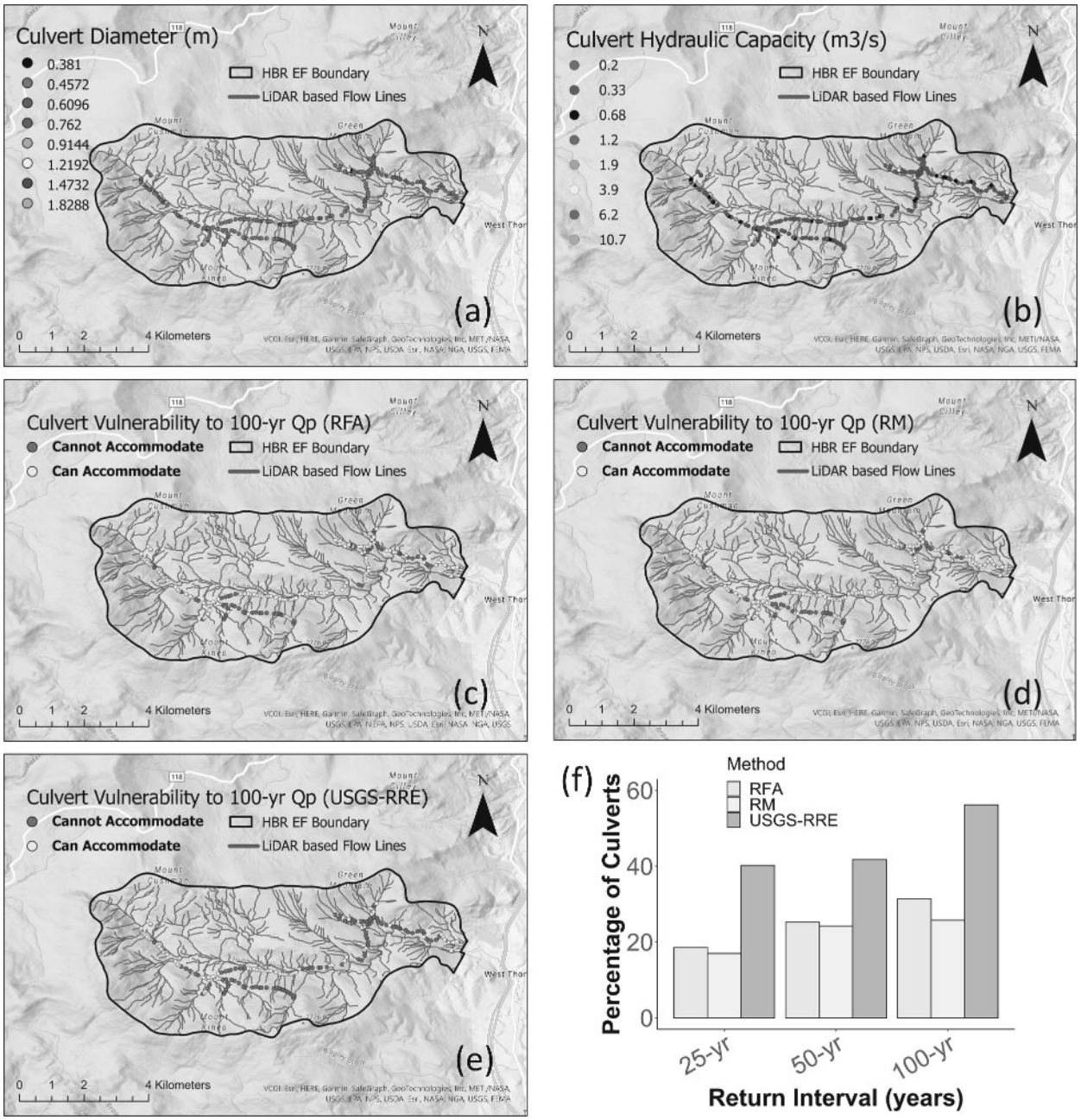

Fig. 8. (a and b) Spatial map showing the culvert's (a) diameter (in meters), and (b) hydraulic capacity (m^3/s), and (c–e) hydrologic vulnerability based on whether they can accommodate the 100-yr Q_p estimated by the (c) RFA, (d) RM, and (e) USGS-RRE, and (f) percentage of culverts (out of 194 culverts) within the HBR EF boundary that fail to accommodate the 25-yr, 50-yr, and 100-yr Q_p estimated by RFA, RM, and USGS-RRE. Note that because the peak discharge estimation was performed for the HUC16-20 watersheds, the parent reference watersheds within HBR are not shown in these maps to avoid any confusion.

undersized. These culverts are considered as hydrologically vulnerable for that flood return period, as shown by red circles.

A higher percentage of road culverts was found to be vulnerable to overtopping based on the Q_p estimated by the USGS-RRE compared to the RFA and RM (Fig. 8f). For example, out of the total 194 culverts, 40 % (or 78 culverts,91 % of which has D = 0.46 m), 42 % (or 83 culverts out of which 86 % has D = 0.46 m, and 12 % has D = 0.61 m), and 56 % (or 109 culverts out of which 1 % has D = 0.38 m, 87 % has D = 0.46 m, and 11 % has D = 0.61 m) of the culverts are vulnerable to 25-year, 50-year, and 100-year Q_p, respectively, estimated with the USGS-RRE (Fig. 8(f), and Table S17). On the other hand, 19 %, 25 %, and 31 % of the culverts are vulnerable based on the 25-year, 50-year, and 100-year Q_p estimated by RFA. Similarly, 17 %, 24 %, and 26 % of the culverts are vulnerable to overtopping based on the 25-year, 50-year and 100-year flood estimated bythe RM. Most of these culverts have D = 0.46 m.

Overall, except for one culvert with diameter of 0.91 m, none of the culverts sized 0.75 m in D or larger were identified as hydrologically vulnerable based on the selected RIs and methods. Therefore, our investigation reveals that replacement of undersized culverts with new ones having a D larger than or equal to 0.75 m is likely to increase flood resiliency of the culverts within the HBR EF. However, these findings are only valid (1) for bank-full conditions where distance between the water level and the center of the culvert, $H = 1.2D$, (2) considering solely the modeled hydrologic vulnerability to overtopping, with no assessment of probability of risk of failure due to exceedance of design discharge

during the intended culvert life span, and (3) assuming no vulnerability to geomorphological risk factors (e.g., sedimentation, bank erosion, siltation, caving, and debris flow), or fish passage requirements are necessary.

An increase in culvert size raises overall installation and material costs of the structure by roughly 14 % on average (Piehl et al., 1988). This additional expense is minor in exchange for a large increase in culvert flow capacity and a 50 % to 75 % reduction in the probability of culvert failure over the physical life of the structure. Therefore, final decision of culvert sizing, and replacement or restoration is assumed to be on a forest manager or engineer who would decide on allowable risks of failure and for costs of restoration based on the culvert's significance and intended life span using an economic cost-benefit analysis (Hansen et al., 2009; Gillespie et al., 2014).

4. Summary and conclusion

This study provides a comprehensive assessment of hydrologic risk from flooding in several gauged and ungauged forested watersheds by implementing advanced statistical and widely used deterministic approaches using the long-term high resolution (15-min) instantaneous streamflow records from multiple United States Department of Agriculture Forest Service (USDA-FS) and United States Geological Survey (USGS) stream gauges and various characteristics of the watersheds draining at those gauged outlets. The objective of this study was threefold: (1) to estimate peak design discharge (Q_p) for 25-year, 50-year and 100-year flood return periods (which are mostly preferred for road culvert design in the national forest lands) based on stationary and non-stationary, probability based at-site frequency analysis (FA) and regional frequency analysis (RFA) for gauged watersheds and transfer that information to the ungauged watersheds, (2) to perform a watershed-scale comparison between the Q_p estimated by FA and RFA and Q_p obtained from the deterministic Rational Method (RM) and semi-empirical USGS regional regression equations (USGS-RRE), and (3) to assess the hydrologic vulnerability of 194 road culverts to overtopping by floods in a pilot EF region, HBR, for which a complete culvert dataset was curated by USDA-FS personnel. To the best of our knowledge, this is the first study that provides a comprehensive multi-approach assessment of hydrologic risks of culvert failure from floods in small, forested headwater watersheds across different climate regions of the US.

The results from this study are rich in watershed scale hydrologic-risk information and can help with an effective assessment for increasing flood resiliency of road culverts in the studied watersheds: 1387 watersheds in the White Mountain National Forest (WMNF) and Hubbard Brook (HBR), and watersheds in multiple other EFs, including three watersheds in HJ Andrews (HJA), two watersheds in Coweeta Hydrologic Lab (CHL), and one watershed each in the Santee (SAN), and Fraser (FRS). The RM outperformed the USGS-RRE in estimating Q_p in the WMNF's smaller watersheds in New Hampshire, and in three other small, high-relief headwater watersheds, including the CHL-WS14 in North Carolina and HJA-WS8 in Oregon. The USGS-RRE, on the other hand, performed better at the larger watersheds, such as Fraser's East Louis (FRS-ELOUI) watershed in Colorado and the SAN-WS80 watershed in South Carolina. Antecedent soil moisture condition was strongly correlated with the annual peak discharges per unit drainage area observed from the HBR-WS3, HBR-WS6, and HBR-WS7 gauging stations which exhibited strong non-stationarity. The USGS-RREs produced substantially higher Q_p estimates and a higher overprediction (larger percentage bias (PB)) for watersheds with a lower percentage of wetland area than the watersheds with a higher percentage of wetland area within the WMNF region. The poor performance of the RM, as expected in the larger watersheds (drainage area $>$ 120-ha), such as SAN-WS80 can be attributed to its large drainage area and high-water storage capacity, supporting earlier results reported by Amatya et al. (2021a–c) for SAN-WS80. In the HBR, a greater number of road culverts were found to be vulnerable to overtopping due to flooding based on the 100-yr flood design discharge estimated by the USGS-RRE as compared to the RFA and RM although USGS-RRE method may overestimate flood design discharge for small watersheds like the one selected in the study.

These results suggest the RFA method provides the least uncertainty in Q_p estimation among the methods studied in EF watersheds for which observed streamflow data from multiple gauges are available to ensure robust information transfer from the gauged to the ungauged watersheds. The results from the hydrologic vulnerability assessment revealed that about 31 %, 26 % and 56 % of the culverts are vulnerable to overtopping due to 100-yr Q_p based on all the three methods, RFA, RM and USGS-RRE, respectively. Almost all the culverts, hydrologically vulnerable to overtopping due to flooding within the HBR EF have a diameter of less than 0.75-m. This finding indicates that replacing undersized culverts with new culverts with a D larger than or equal to 0.75 m can provide some insurance in the face of increasing extreme precipitation events within the HBR EF. However, these findings are only valid for bank-full conditions and/or where distance between the water level and the center of the culvert, $H = 1.2D$, and locations where the structure is not prone to geomorphological vulnerability (such as sedimentation, bank erosion, siltation, caving, and debris flow) and permits aquatic organism passage. It is important to note that the design discharge estimated for the rest of the watersheds with RSCs in the WMNF can be used in the near future for hydrologic vulnerability assessment of the road culverts as and when the culvert data becomes available.

There are several logical extensions to the vulnerability assessment described in this article. Evaluation of hydraulic capacity in the presence of large woody debris is an important factor in forested watersheds that is missing in the current analysis. Integrating hydrologic vulnerability with a geomorphological vulnerability assessment would provide a more comprehensive and reliable assessment. In addition, design flood exceedance probability-based failure risk assessment of culverts over their intended life span used in economic cost-benefit analysis was also left for future studies. As a result, the findings of these case studies should be evaluated with caution and by incorporating present field conditions before undertaking design initiatives or projecting them to other similar watersheds. Relief culverts primarily provides road-side ditch-drainage relief and hydrologic connectivity through cross-drainage, therefore, special care should be taken to isolate and treat the hydrologic vulnerability of relief culverts differently from the other culverts draining a specific upland area. The methodology used in the hydrologic vulnerability assessment of culverts can be replicated for other EF regions as and when culvert data becomes available. Further improvements are possible with the estimation of Q_p using a continuous simulation approach that tracks the soil moisture dynamics (Winter et al., 2019) which can reduce uncertainties in Q_p estimates for watersheds with high water retention capability. Similarly, model parameters determined directly on the basis of physiographic characteristics of catchments that are able to simulate the rainfall losses and the dynamics of runoff formation taking into account the spatial variability of the catchment, can lead to further improvements of the results (Petroselli and Grimaldi, 2018; Młyński et al., 2020). Precipitation-intensity-frequency-duration estimates for future time-periods, developed using the Coupled Model Intercomparison Project Phase 6 outputs, can be used in estimating Q_p for designing possible climate change resilient culverts as another future scope of this study (Jalowska et al., 2021).

Overall, the results from this study can be useful for strategically investing in road-stream crossing re-designing and installations. This will foster flood resiliency that has the potential to reduce the economic and societal costs through reduced failure rates and lower maintenance costs while maintaining important ecological values of the forested watersheds. However, it is worth mentioning that engineers must carefully select the most appropriate design strategy for developing new and renovated roads depending on government criteria (USDOT, 2012, 2018) and proper engineering judgment for the specific watershed and drainage culverts. After completion of the design, careful consideration

should also be given to the proposed installation procedures for the drainage culvert, such as checking for alignment, stream dimension, and substrate composition (Hansen et al., 2009). Finally, developing and implementing effective monitoring procedures and strategies for the drainage culverts will maintain its flood resiliency throughout the life of the structure.

CRediT authorship contribution statement

Sourav Mukherjee: Conceptualization, Data curation, Formal analysis, Investigation, Methodology, Software, Validation, Visualization, Writing – original draft. **Devendra M. Amatya:** Conceptualization, Funding acquisition, Methodology, Project administration, Resources, Supervision, Writing – review & editing. **John L. Campbell:** Resources, Writing – review & editing. **Landon Gryczkowski:** Resources, Writing – review & editing, Data curation. **Sudhanshu Panda:** Supervision, Writing – review & editing. **Sherri L. Johnson:** Resources, Writing – review & editing. **Kelly Elder:** Resources, Writing – review & editing. **Anna M. Jalowska:** Writing – review & editing. **Peter Caldwell:** Resources, Writing – review & editing. **Johnny M. Grace:** Writing – review & editing. **Dariusz Młyński:** Writing – review & editing. **Andrzej Wałęga:** Writing – review & editing.

Declaration of competing interest

The authors declare that they have no known competing financial interests or personal relationships that could have appeared to influence the work reported in this paper.

Data availability

Data will be made available on request.

Acknowledgements

This study was supported by a funding agreement (#18IA11330155072) between the USDA Forest Service and the Oak Ridge Institute for Science and Education (ORISE). We are thankful for the streamflow data provided by USDAFS researchers, Dr. Nina Lany at the Hubbard Brook EF, Dr. Chris Oishi at the Coweeta Hydrology Laboratory, and Charles A. Harrison at the Santee EF, and Banning Starr and Laurie Porth at the Fraser Experimental Forest. We thank technicians, Ian Halm, Hannah Vollmer and Gabe Winant for providing the culvert dataset for the Hubbard Brook EF. The USGS provided streamflow data and NOAA provided hourly precipitation data and storm design precipitation intensities. We would like to gratefully acknowledge the help of Shawna Reid at the USDAFS Southern Research Station, for acquiring the geospatial dataset of watersheds and related information about road-stream crossings and road networks located across the EFs in this study. We also thank Karl Buchholz at the Francis Marion National Forest, SC, and Stephanie Laseter and Johnny Boggs, both at the USDAFS Southern Research Station, for their support. The opinions presented in this article are those of the authors and should not be construed to represent any official USDA or US Government determination or policy. Similarly, the views expressed in this article are those of the authors and do not necessarily represent the views or the policies of the U.S. Environmental Protection Agency.

Appendix A. Supplementary data

Supplementary data to this article can be found online at https://doi.org/10.1016/j.jhydrol.2024.130698.

References

Alexander, R.R., Watkins, R.K., 1977. The Fraser Experimental Forest. Department of Agriculture, Forest Service, Rocky Mountain Forest and Range, Colorado.
Amatya, D., Ssegane, H., Trettin, C., Hamidi, M.D., 2021. Hydrologic relationships of a paired coastal watershed on the santee experimental forest for evaluating watershed-scale effects of longleaf pine restoration on water yield.
Amatya, D.M., Herbert, S., Trettin, C.C., Hamidi, M.D., Amatya, D.M., 2021a. Evaluation of paired watershed runoff relationships since recovery from a major hurricane on a coastal forest—a basis for examining effects of Pinus palustris restoration on water yield. Water 13 (23), 3121. https://doi.org/10.3390/w13213121.
Amatya, D.M., Walega, A., 2020. Long-term data–the key for evaluating runoff peak discharge estimation tools and parameters for watersheds on forest lands. Adv. Civil Eng. Technol. 4 (2).
Amatya, D.M., Campbell, J., Wohlgemuth, P., Elder, K., Sebestyen, S., Johnson, S., Keppeler, E., Adams, M.B., Caldwell, P., Misra, D., 2016. Hydrological processes of reference watersheds in experimental forests, USA. In: Forest hydrology: Processes, management and assessment. Cabi, Wallingford UK, pp. 219–239.
Amatya, D.M., Williams, T.M., Nettles, J.E., Skaggs, R.W., Trettin, C.C., 2019. Comparison of hydrology of two Atlantic coastal plain forests. Trans. ASABE 62 (6), 1509–1529.
Amatya, D.M., Tian, S., Marion, D.A., Caldwell, P., Laseter, S., Youssef, M.A., Grace, J.M., Chescheir, G.M., Panda, S., Ouyang, Y., Sun, G., 2021b. Estimates of precipitation IDF curves and design discharges for road-crossing drainage structures: case study in four small forested watersheds in the Southeastern US. J. Hydrol. Eng. 26 (4), 05021004.
Beier, C.M., Caputo, J., Groffman, P.M., 2015. Measuring ecosystem capacity to provide regulating services: forest removal and recovery at Hubbard Brook (USA). Ecol. Appl. 25 (7), 2011–2021.
Beneyto, C., Aranda, J.Á., Benito, G., Francés, F., 2020. New approach to estimate extreme flooding using continuous synthetic simulation supported by regional precipitation and non-systematic flood data. Water 12 (11), 3174.
Berghuijs, W.R., Woods, R.A., Hutton, C.J., Sivapalan, M., 2016. Dominant flood generating mechanisms across the United States. Geophys. Res. Lett. 43 (9), 4382–4390. https://doi.org/10.1002/2016GL068070.
Beven, K.J., 2011. Rainfall-Runoff Modelling: The Primer. John Wiley & Sons.
Bonnin, G., Martin, D., Lin, B., Parzybok, T., Yekta, M., Riley, D., 2006. Precipitation-frequency atlas of the United States. Volume 3 Version 4.0. Puerto Rico and the US Virgin Islands.
Boughton, W.C., 1989. A review of the USDA SCS curve number method. Soil Res. 27 (3), 511–523.
Buto, S.G., Anderson, R.D., 2020. NHDPlus High Resolution (NHDPlus HR)—A Hydrography Framework for the Nation. US Geological Survey.
Caldwell, P.V., Miniat, C.F., Elliott, K.J., Swank, W.T., Brantley, S.T., Laseter, S.H., 2016. Declining water yield from forested mountain watersheds in response to climate change and forest mesophication. Glob. Chang. Biol. 22 (9), 2997–3012. https://doi.org/10.1111/gcb.13309.
Campbell, J.L., Driscoll, C.T., Pourmokhtarian, A., Hayhoe, K., 2011. Streamflow responses to past and projected future changes in climate at the Hubbard Brook Experimental Forest, New Hampshire, United States. Water Resour. Res. 47 (2).
Campbell, J.L., Rustad, L.E., Bailey, S.W., Bernhardt, E.S., Driscoll, C.T., Green, M.B., Rosi, E.J., 2021. Watershed studies at the Hubbard brook experimental forest: building on a long legacy of research with new approaches and sources of data. Hydrol. Process. 35, 14016. https://doi.org/10.1002/hyp.14016.
Capesius, J.P., Stephens, V.C., 2009. Regional Regression Equations for Estimation of Natural Streamflow Statistics in Colorado. US Department of the Interior, US Geological Survey.
Cea, L., Fraga, I., 2018. Incorporating antecedent moisture conditions and intraevent variability of rainfall on flood frequency analysis in poorly gauged basins. Water Resour. Res. 54 (11), 8774–8791.
Chang, H., Lafrenz, M., Jung, I.W., Figliozzi, M., Platman, D., Pederson, C., 2010. Potential impacts of climate change on flood-induced travel disruptions: a case study of Portland, Oregon, USA. Ann. Assoc. Am. Geogr. 100 (4), 938–952.
Coles, S., Bawa, J., Trenner, L., Dorazio, P., 2001. An Introduction to Statistical Modeling of Extreme Values. Springer, London.
Corbin, J., Morgan, H., Patrohay, E., Williams, T., Amatya, D., Darnault, C.J., 2021. Hydrologic modeling of urban development scenarios and low-impact design systems on an undisturbed coastal forested watershed under extreme rainfall-runoff events and hydro-meteorological conditions in a changing climate. J. South Carolina Water Resour. 8 (2), 7.
Dalrymple, T., 1960. Flood-Frequency Analyses. US Government Printing Office.
Darestani, Y.M., Webb, B., Padgett, J.E., Pennison, G., Fereshtehnejad, E., 2021. Fragility analysis of coastal roadways and performance assessment of coastal transportation systems subjected to storm hazards. J. Perform. Constr. Facil 35 (6), 04021088.
David, G.C.L., 2011. Characterizing Flow Resistance in High Gradient Mountain Streams, Fraser Experimental Forest, Colorado. Colorado State University (Doctoral dissertation).
De Michele, C.A., Salvadori, G., 2002. On the derived flood frequency distribution: analytical formulation and the influence of antecedent soil moisture condition. J. Hydrol. 262 (1–4), 245–258.
Eisenbies, M.H., Aust, W.M., Burger, J.A., Adams, M.B., 2007. Forest operations, extreme flooding events, and considerations for hydrologic modeling in the Appalachians—a review. For. Ecol. Manage. 242 (2–3), 77–98.
El Adlouni, S., Ouarda, T.B.M.J., Zhang, X., Roy, R., Bobée, B., 2007. Generalized maximum likelihood estimators for the nonstationary generalized extreme value

model. Water Resour. Res. 43, W03410. https://doi.org/10.1029/2005WR004545, 13 pp.
Fang, X., Pomeroy, J.W., 2016. Impact of antecedent conditions on simulations of a flood in a mountain headwater basin. Hydrol. Process. 30 (16), 2754–2772.
Feaster, T.D., Gotvald, A.J., Weaver, J.C., 2014. Estimating flood magnitude and frequency for urban and small, rural streams in Georgia, South Carolina, and North Carolina, 2011 (No. 2014-3015). US Geological Survey.
Fleming, G., Franz, D.D., 1971. Flood frequency estimating techniques for small watersheds. J. Hydraulics Division 97 (9), 1441–1460.
Folmar, N.D., Miller, A.C., Woodward, D.E., 2007. History and development of the NRCS lag time equation 1. JAWRA J. Am. Water Resour. Assoc. 43 (3), 829–838.
Franzini, J.B., Finnemore, E.J., 1997. Fluid mechanics with engineering applications. (ninth ed.9 ed.), McGraw-Hill, New York.
Fredriksen, R.L., 1970. Erosion and sedimentation following road construction and timber harvest on unstable soils in three small western Oregon watersheds. Pacific Northwest Forest and Range Experiment Station, U.S. Department of Agriculture.
Gaume, E., Gaál, L., Viglione, A., Szolgay, J., Kohnová, S., Blöschl, G., 2010. Bayesian MCMC approach to regional flood frequency analyses involving extraordinary flood events at ungauged sites. J. Hydrol. 394 (1–2), 101–117.
Genereux, D.P., 2003. Comparison of methods for estimation of 50-year peak discharge from a small, rural watershed in North Carolina. Environ. Geol. 44, 53–58.
Gillespie, N., Unthank, A., Campbell, L., Anderson, P., Gubernick, R., Weinhold, M., Rowan, J., 2014. Flood effects on road–stream crossing infrastructure: economic and ecological benefits of stream simulation designs. Fisheries 39 (2), 62–76.
Glasser, S.P., 2005. History of watershed management in the US Forest Service: 1897–2005. J. For. 103 (5), 255–258.
Gochis, D., Schumacher, R., Friedrich, K., Doesken, N., Kelsch, M., Sun, J., Ikeda, K., Lindsey, D., Wood, A., Dolan, B., Matrosov, S., 2015. The great Colorado flood of September 2013. Bull. Am. Meteorol. Soc. 96 (9), 1461–1487.
Goodman, A.C., Segura, C., Jones, J.A., Swanson, F.J., 2023. Seventy years of watershed response to floods and changing forestry practices in western Oregon, USA. Earth Surface Processes and Landforms, Advance online publication.
Grimaldi, S., Volpi, E., Langousis, A., Papalexiou, SM., De Luca, D.L., Piscopia, R., Nerantzaki, S.D., Papacharalampous, G., Petroselli A., 2022. Continuous hydrologic modelling for small and ungauged basins: a comparison of eight rainfall models for sub-daily runoff simulations. J. Hydrol. 610:127866.
Grimaldi, S., Petroselli, A., 2015a. Do we still need the rational formula? An alternative empirical procedure for peak discharge estimation in small and ungauged basins. Hydrol. Earth Syst. Sci. 19 (1), 67–77. https://doi.org/10.1080/02626667.2014.880546.
Grimaldi, S., Petroselli, A., 2015b. Do we still need the rational formula? An alternative empirical procedure for peak discharge estimation in small and ungauged basins. Hydrol. Sci. J. 60 (1), 67–77.
Grimaldi, S., Nardi, F., Piscopia, R., Petroselli, A., Apollonio, C., 2021. Continuous hydrologic modeling for design simulation in small and ungauged basins: a step forward and some tests for its practical use. J. Hydrol. 595, 125664.
Halbert, K., Nguyen, C.C., Payrastre, O., Gaume, E., 2016. Reducing uncertainty in flood frequency analyses: a comparison of local and regional approaches involving information on extreme historical floods. J. Hydrol. 541, 90–98.
Hansen, B., Nieber, J.L., Lenhart, C., 2009. Cost analysis of alternative culvert installation practices in Minnesota.
Hansen, W.F., 1987. Some applications of flood frequency and risk information in forest management. In: V. P. Singh (ed.), Application of Frequency and Risk in Water Resources, 219-226. 1987 by D. Reidel Publishing Company.
Harder, S.V., Amatya, D.M., Callahan, T.J., Trettin, C.C., Hakkila, J., 2007. Hydrology and water budget for a forested Atlantic coastal plain watershed, South Carolina 1. J. Am. Water Resour. Assoc. 43 (3), 563–575. https://doi.org/10.1111/j.1752-1688.2007.00035.x.
Hayes, D.C., Young, R.L., 2006. Comparison of peak discharge and runoff characteristic estimates from the rational method to field observations for small basins in central Virginia. No. 2005-5254. 2006.
Heredia, N., Roper, B., Gillespie, N., Roghair, C., 2016. Technical guide for field practitioners: Understanding and monitoring aquatic organism passage at road stream crossings. Technical Rep. No. TR-101. Washington, DC: USDA, Forest Service, National Stream and Aquatic Ecology Center.
Hosking, J.R., 1990. L-moments: analysis and estimation of distributions using linear combinations of order statistics. J. R. Stat. Soc. Ser. B Stat Methodol. 52 (1), 105–124.
Hosking, J.R.M., Wallis, J.R., 1997. Regional frequency analysis (p. 240).
Hosking, J.R., 2022. Regional frequency analysis using L-moments. R package, version 3.4. https://CRAN.R-project.org/package=lmomRFA.
Jakob, M., Mark, E., McDougall, S., Friele, P., Lau, C.-A., Bale, S., 2020. Regional debris-flow and debris-flood frequency–magnitude relationships. Earth Surf. Proc. Land. 45, 2954–2964. https://doi.org/10.1002/esp.4942.
Jakob, M., Davidson, S., Bullard, G., Busslinger, M., Collier-Pandya, B., Grover, P., Lau, C.A., 2022. Debris-flood hazard assessments in steep streams. Water Resour. Res. 58 (4) e2021WR030907.
Jalowska, A.M., Spero, T.L., Bowden, J.H., 2021. Projecting changes in extreme rainfall from three tropical cyclones using the design-rainfall approach. NPJ Clim. Atmos. Sci. 4, 1–8. https://doi.org/10.1038/s41612-021-00176-9.
Johnson, S.L., Swanson, F.J., Grant, G.E., Wondzell, S.M., 2000. Riparian Forest disturbances by a mountain flood—the influence of floated wood. Hydrol. Process. 14 (16–17), 3031–3050.
Johnson, S.L., Henshaw, D., Downing, G., Wondzell, S., Schulze, M., Kennedy, A., Jones, J.A., 2021. Long-term hydrology and aquatic biogeochemistry data from H. J. Andrews Experimental Forest, Cascade Mountains Oregon. Hydrol. Process 35, e14187.
Ke, Q., Tian, X., Bricker, J., Tian, Z., Guan, G., Cai, H., Huang, X., Yang, H., Liu, J., 2020. Urban pluvial flooding prediction by machine learning approaches–a case study of Shenzhen city, China. Adv. Water Resour. 145, 103719.
Keller, G., Ketcheson, G., 2011. Storm damage risk reduction: storm proofing low-volume roads. Transp. Res. Rec. 2203 (1), 211–218.
Keller, G., Sherar, J., 2003. Low-volume roads engineering: Best management practices. Transp. Res. Rec. 1819 (1), 174–181.
Kendall, M.G., 1975. Rank Correlation Methods. Oxford University Press, New York, NY.
Kiah, R.G., Stasulis, N.W., 2018. Preliminary Stage and Streamflow Data at Selected US Geological Survey Streamgages in Maine and New Hampshire for the Flood of October 30–31, 2017. US Geological Survey.
Kim, H., Shin, J.Y., Kim, T., Kim, S., Heo, J.H., 2020. Regional frequency analysis of extreme precipitation based on a nonstationary population index flood method. Adv. Water Resour. 146, 103757.
Kirschbaum, D., Kapnick, S.B., Stanley, T., Pascale, S., 2020. Changes in extreme precipitation and landslides over High Mountain Asia. e2019GL085347 Geophys. Res. Lett. 47. https://doi.org/10.1029/2019GL085347.
Kuichling, E., 1889. The relation between the rainfall and the discharge of sewers in populous districts. Trans. Am. Soc. Civ. Eng. 20 (1), 1–56.
Laio, F., 2004. Cramer–von Mises and Anderson-Darling goodness of fit tests for extreme value distributions with unknown parameters. Water Resour. Res. 40 (9).
Laseter, S.H., Ford, C.R., Vose, J.M., Swift Jr., L.W., 2012. Long-term temperature and precipitation trends at the Coweeta hydrologic laboratory, Otto, North Carolina, USA. Hydrol. Res. 43, 890–901. https://doi.org/10.2166/nh.2012.067.
Levin, S.B., Sanocki, C.A., 2023. Estimating flood magnitude and frequency for unregulated streams in Wisconsin. US Geological Survey.
Likens, G.E., 2013. Biogeochemistry of a Forested Ecosystem. Springer, New York.
Magilligan, F.J., James, L.A., Lecce, S.A., Dietrich, J.T., Kupfer, J.A., 2019. Geomorphic responses to extreme rainfall, catastrophic flooding, and dam failures across an urban to rural landscape. Ann. Am. Assoc. Geogr. 109 (3), 705–729.
Malcom, R., 1989. Elements of Stormwater Design. Civil Engineering Department, North Carolina State University, Raleigh, NC (Unpublished report).
Mamo, T.G., 2015. Evaluation of the potential impact of rainfall intensity variation due to climate change on existing drainage infrastructure. J. Irrig. Drain. Eng. 141 (10), 05015002.
Mann, H.B., 1945. Nonparametric tests against trend. Econometrica 13, 245–259. https://doi.org/10.2307/1907187.
Marciano, C.G., Lackmann, G.M., 2017. The South Carolina Flood of October 2015: Moisture Transport Analysis and the Role of Hurricane Joaquin. J. Hydrometeorol. 18 (11), 2973–2990. https://doi.org/10.1175/JHM-D-16-0235.1.
Marion, D.A., 2004. An improved flood-frequency model for small watersheds in the upper Ouachita Mountains. In: Ouachita and Ozark Mountains Symposium: Ecosystem Management Research: Hot Springs, Arkansas, October 26-28, 1999 (No. 74, p. 207). Southern Research Station.
McCullagh, P., Nelder, J., 1989. Generalized Linear Models. Chapman & Hall/CRC, London.
McEnroe, B.M., Young, C.B., Williams, A.R., Hinshaw, M., 2013. Estimating Design Discharges for Drainage Structures in Western Kansas. Dept. of Transportation. Bureau of Materials & Research, Kansas.
Megnounif, A., Terfous, A., Ouillon, S., 2013. A graphical method to study suspended sediment dynamics during flood events in the Wadi Sebdou, NW Algeria (1973–2004). J. Hydrol. 497, 24–36.
Merz, R., Blöschl, G., 2009. A regional analysis of event runoff coefficients with respect to climate and catchment characteristics in Austria. Water Resour. Res. 45 (1).
Mishra, A., Alnahit, A., Campbell, B., 2021. Impact of land uses, drought, flood, wildfire, and cascading events on water quality and microbial communities: a review and analysis. J. Hydrol. 596, 125707.
Mishra, A., Mukherjee, S., Merz, B., Singh, V.P., Wright, D.B., Villarini, G., Paul, S., Kumar, D.N., Khedun, C.P., Niyogi, D., Schumann, G., 2022. An overview of flood concepts, challenges, and future directions. J. Hydrol. Eng. 27 (6), 03122001.
Mitchell, J.N., Wagner, D.M., Veilleux, A.G., 2023. Magnitude and frequency of floods on Kaua'i, O'ahu, Moloka'i, Maui, and Hawai'i, State of Hawai'i, based on data through water year 2020. US Geological Survey.
Mizukami, N., Rakovec, O., Newman, A.J., Clark, M.P., Wood, A.W., Gupta, H.V., Kumar, R., 2019. On the choice of calibration metrics for "high-flow" estimation using hydrologic models. Hydrol. Earth Syst. Sci. 23 (6), 2601–2614.
Młyński, D., Wałęga, A., Ozga-Zieliński, B., Ciupak, M., Petroselli, A., 2020. New approach for determining the quantiles of maximum annual flows in ungauged catchments using the EBA4SUB model. J. Hydrol. 589, 125198 https://doi.org/10.1016/j.jhydrol.2020.125198.
Montanari, A., Koutsoyiannis, D., 2014. Modeling and mitigating natural hazards: stationarity is immortal! Water Resour. Res. 50 (12), 9748–9756.
Mukherjee, S., Amatya, D.M., Jalowska, A.M., Campbell, J.L., Johnson, S.L., Elder, K., Panda, S., Grace, J.M., Kikoyo, D., 2023. Comparison of on-site versus NOAA's extreme precipitation intensity-duration-frequency estimates for six forest headwater catchments across the continental United States. Stoch. Env. Res. Risk A 37 (10), 4051–4070.
Ngongondo, C.S., Xu, C.-Y., Tallaksen, L.M., Alemaw, B., Chirwa, T., 2011. Regional frequency analysis of rainfall extremes in Southern Malawi using the index rainfall and L-moments approaches. Stoch Environ. Res. Risk Assess 25, 939–955. https://doi.org/10.1007/s00477-011-0480-x.
O'Brien, N.L., Burn, D.H., 2014. A nonstationary index-flood technique for estimating extreme quantiles for annual maximum streamflow. J. Hydrol. 519, 2040–2048.

ODOT (Oklahoma DOT). (2014). "Hydrology." Chap. 7 in Roadway drainage design manual. Oklahoma City, OK: ODOT.

Olson, S.A., Bent, G.C., 2013. Annual Exceedance Probabilities of the Peak Discharges of 2011 at Streamgages in Vermont and Selected Streamgages in New Hampshire, Western Massachusetts, and Northeastern New York. US Department of the Interior, US Geological Survey: Reston, VA. DOI: 10.3133/sir20135187.

Olson, S.A., 2008. Estimation of flood discharges at selected recurrence intervals for streams in New Hampshire (No. FHWA-NH-RD-14282F). New Hampshire. Dept. of Transportation.

Panda, S.S., Amatya, D.M., Grace, J.M., Caldwell, P., Marion, D.A., 2022. Extreme precipitation-based vulnerability assessment of road-crossing drainage structures in forested watersheds using an integrated environmental modeling approach. Environ. Model. Softw. 155, 105413.

Papalexiou, S.M., Montanari, A., 2019. Global and regional increase of precipitation extremes under global warming. Water Resour. Res. 55, 4901–4914. https://doi.org/10.1029/2018WR024067.

Pathiraja, S., Westra, S., Sharma, A., 2012. Why continuous simulation? The role of antecedent moisture in design flood estimation. Water Resour. Res. 48 (6).

Pegram, G., Parak, M., 2004. A review of the regional maximum flood and rational formula using geomorphological information and observed floods. Water SA 30 (3), 377–392.

Perica, S., Pavlovic, S., St Laurent, M., Trypaluk, C., Unruh, D., Martin, D., Wilhite, O., 2015. Precipitation-Frequency Atlas of the United States. Volume 10, Version 3.0. Northern States; Connecticut, Maine, Massachusetts, New Hampshire, New York, Rhode Island, Vermont.

Perica, S., Pavlovic, S., St Laurent, M., Trypaluk, C., Unruh, D., Wilhite, O., 2018. Precipitation-frequency atlas of the United States. Volume 11, Version 2.0. Texas.

Petroselli, A., Grimaldi, S., 2018. Design hydrograph estimation in small and fully ungauged basins: a preliminary assessment of the EBA4SUB framework. J. Flood Risk Manage. 11, S197–S210.

Piehl, B.T., Pyles, M.R., Beschta, R.L., 1988. Flow capacity of culverts on Oregon coast range forest roads 1. JAWRA J. Am. Water Resour. Assoc. 24 (3), 631–637.

Pregnolato, M., Ford, A., Wilkinson, S.M., Dawson, R.J., 2017. The impact of flooding on road transport: a depth-disruption function. Transp. Res. Part D: Transp. Environ. 55, 67–81.

Read, L.K., Vogel, R.M., 2015. Reliability, return periods, and risk under nonstationarity. Water Resour. Res. 51, 6381–6398. https://doi.org/10.1002/2015WR017089.

Rootzén, H., Katz, R.W., 2013. Design life level: quantifying risk in a changing climate. Water Resour. Res. 49 (9), 5964–5972.

Ross, C.W., Prihodko, L., Anchang, J., Kumar, S., Ji, W., Hanan, N.P., 2018. HYSOGs250m, global gridded hydrologic soil groups for curve-number-based runoff modeling. Sci. Data 5, 180091. https://doi.org/10.1038/sdata.2018.91.

Seddon, N., Smith, A., Smith, P., Key, I., Chausson, A., Girardin, C., House, J., Srivastava, S., Turner, B., 2021. Getting the message right on nature-based solutions to climate change. Glob. Chang. Biol. 27 (8), 1518–1546.

Sörensen, R., Zinko, U., Seibert, J., 2006. On the calculation of the topographic wetness index: evaluation of different methods based on field observations. Hydrol. Earth Syst. Sci. 10 (1), 101–112.

Srivastava, A., Grotjahn, R., Ullrich, P.A., Risser, M., 2019. A unified approach to evaluating precipitation frequency estimates with uncertainty quantification: application to Florida and California watersheds. J. Hydrol. 578, 124095 https://doi.org/10.1016/j.jhydrol.2019.124095.

St. George, S., Mudelsee, M., 2019. The weight of the flood-of-record in flood frequency analysis. J. Flood Risk Manage. 12, e12512.

Tedela, N.H., McCutcheon, S.C., Rasmussen, T.C., Hawkins, R.H., Swank, W.T., Campbell, J.L., Tollner, E.W., 2012. Runoff curve numbers for 10 small forested watersheds in the mountains of the eastern United States. J. Hydrol. Eng. 17 (11), 1188–1198.

Teng, J., Jakeman, A.J., Vaze, J., Croke, B.F., Dutta, D., Kim, S.J., Bale, S., 2017. Flood inundation modeling: a review of methods, recent advances, and uncertainty analysis. Environ. Model. Softw. 90, 201–216.

Thomas, R.Q., Hurtt, G.C., Dubayah, R., Schilz, M.H., 2008. Using lidar data and a height-structured ecosystem model to estimate forest carbon stocks and fluxes over mountainous terrain. Can. J. Remote. Sens. 34 (sup2), S351–S363.

Thompson, D.B., 2006. The Rational Method, Regional Regression Equations, and Site Specific Flood-Frequency Relations. Texas DOT, Austin, TX.

Thompson, D.B., 2004. Literature review for TxDOT project 0–4405: Scale issues in hydrology. TxDOT Report 0–4405–1, TechMRT, Texas Tech University, Lubbock, Texas 79409.

Trommer, J., Loper, J., Hammett, K., 1996. Evaluation and Modification of Five Techniques for Estimating Stormwater Runoff for Watersheds in West-Central Florida. US Department of the Interior, USGS, Reston, VA.

USDA, 2021. Estimation Runoff Volume and Peak Discharge. Chapter 2, part 650. Engineering Field Handbook, Title 201 National Engineering Handbook, United States Department of Agriculture (USDA) Natural Resources Conservation Service, Washington, D.C. USA, pp 1-43.

USDOT, 2012. Evaluating scour at bridges. Hydraulic Engineering Circular No. 18, Publication No. FHWA-HIF-12-003. Washington, DC: Federal Highway Administration, USDOT.

USDOT, 2018. US Forest Service transportation resiliency guidebook: Addressing climate change impacts on US Forest Service transportation assets. Cambridge, MA: USDOT John A. Volpe National Transportation Systems Center in Cambridge.

Van Dam, B.R., Crosswell, J.R., Paerl, H.W., 2018. Flood-driven CO2 emissions from adjacent North Carolina estuaries during Hurricane Joaquin (2015). Mar. Chem. 207, 1–2.

Viglione, A., Blöschl, G., 2009. On the role of storm duration in the mapping of rainfall to flood return periods. Hydrol. Earth Syst. Sci. 13 (2), 205–216.

Viglione, A., Hosking, J.R., Laio, F., Miller, A., Gaume, E., Payrastre, O., Viglione, M.A., 2020. Package 'nsRFA'. Non-supervised Regional Frequency Analysis. CRAN Repository.

Vogel, R.M., Castellarin, A., 2017. Risk, reliability, and return periods and hydrologic design. In: Handbook of Applied Hydrology; Singh, VP, Ed.; McGraw-Hill Book Company: New York, NY, USA.

Vogel, R.M., Wilson, I., Daly, C., 1999. Regional regression models of annual streamflow for the United States. J. Irrig. Drain. Eng. 125 (3), 148–157.

Walder, J.S., O'Connor, J.E., 1997. Methods for predicting peak discharge of floods caused by failure of natural and constructed earthen dams. Water Resour. Res. 33 (10), 2337–2348.

Walega, A., Amatya, D.M., Caldwell, P., Marion, D., Panda, S., 2020. Assessment of storm direct runoff and peak flow rates using improved SCS-CN models for selected forested watersheds in the Southeastern United States. J. Hydrol.: Reg. Stud. 27, 100645 https://doi.org/10.1016/j.ejrh.2019.100645.

Ward, P.J., Blauhut, V., Bloemendaal, N., Daniell, J.E., de Ruiter, M.C., Duncan, M.J., Kirschbaum, D., 2020. Natural hazard risk assessments at the global scale. Nat. Hazards Earth Syst. Sci. 20 (4), 1069–1096.

Wasko, C., Nathan, R., Peel, M.C., 2020. Changes in antecedent soil moisture modulate flood seasonality in a changing climate. Water Resour. Res. 56 (3) e2019WR026300.

Weaver, W.E., Hagans, D.K., 1994. Handbook for forest and ranch roads: A guide for planning, designing, constructing, reconstructing, maintaining and closing wildland roads. Washington, DC: Pacific Watershed Associates for Mendocino County Resource Conservation District in Cooperation with California Department of Forestry and Fire Protection and the USDA Soil Conservation Service.

Weaver, J., Feaster, T.D., Gotvald, A.J., 2009. Magnitude and Frequency of Rural Floods in the Southeastern United States, through 2006, vol. 2. U. S. Geological Survey, North Carolina.

Winter, B., Schneeberger, K., Dungc, N.V., Huttenlaud, M., Achleitnere, S., Stöttera, J., Vorogushyn, S., 2019. A continuous modelling approach for design flood estimation on sub-daily time scale. Hydrol. Sci. J. 64(5), 539–554. 10.1080/02626667.2019.1593419.

Wright, D.B., Bosma, C.D., Lopez-Cantu, T., 2019. US hydrologic design standards insufficient due to large increases in frequency of rainfall extremes. Geophys. Res. Lett. 46 (14), 8144–8153.

Yellen, B., Woodruff, J.D., Cook, T.L., Newton, R.M., 2016. Historically unprecedented erosion from Tropical Storm Irene due to high antecedent precipitation. Earth Surf. Process. Landforms 41 (4), 677–684. https://doi.org/10.1002/esp.3896.

Yochum, S.E., Scott, J.A., Levinson, D.H., 2019. Methods for assessing expected flood potential and variability: Southern Rocky Mountains region. Water Resour. Res. 55, 6392–6416. https://doi.org/10.1029/2018WR024604.